

# Lindblad master equation approach to the dissipative quench dynamics of planar superconductors

Andrea Nava<sup>(1)</sup>, Carmine Antonio Perroni<sup>(2)</sup>, Reinhold Egger<sup>(1)</sup>, Luca Lepori<sup>(3)</sup>, and Domenico Giuliano<sup>(4)</sup>

<sup>(1)</sup>*Institut für Theoretische Physik,*

*Heinrich-Heine-Universität, 40225 Düsseldorf, Germany*

<sup>(2)</sup>*Dipartimento di Fisica “E. Pancini” Complesso Universitario Monte S. Angelo Via Cintia,*  
*I-80126 Napoli, Italy and*

*CNR-SPIN, Complesso Universitario Monte S. Angelo Via Cintia,*

*I-80126 Napoli, Italy and*

*I.N.F.N., Sezione di Napoli,*

*Complesso Universitario Monte S. Angelo Via Cintia,*

*I-80126 Napoli, Italy*

<sup>(3)</sup>*Dipartimento di Scienze Matematiche Fisiche e Informatiche Università di Parma and*

*INFN, Gruppo Collegato di Parma,*

*Parco Area delle Scienze 7/A, 43124, Parma, Italy.*

<sup>(4)</sup>*Dipartimento di Fisica,*

*Università della Calabria Arcavacata di Rende I-87036,*

*Cosenza, Italy and*

*I.N.F.N., Gruppo collegato di Cosenza Arcavacata di Rende I-87036, Cosenza, Italy*

(Dated: November 27, 2023)

We employ the Lindblad master equation method to study the nonequilibrium dynamics following a parametric quench in the Hamiltonian of an open, two-dimensional superconducting system coupled to an external bath. Within our approach we show how, in the open system, the dissipation works as an effective stabilization mechanism in the time evolution of the system after the quench. Eventually, we evidence how the mismatch between the phases corresponding to the initial and to the final state of the system determines a dynamical phase transition between the two distinct phases. Our method allows for fully characterizing the dynamical phase transition in an open system in several cases of physical relevance, by means of a combined study of the time-dependent superconducting gap and of the fidelity between density matrices.

## I. INTRODUCTION

Related to the continuous developments of time-resolved spectroscopic investigation methods in many-particle systems, there has recently been an increasing interest in nonequilibrium correlated systems. For instance, using time-dependent angle-resolved spectroscopy, it becomes possible to investigate the different time evolutions of quasiparticle states in a superconductor in different regions of the Brillouin zone, together with the corresponding effects on the dependence in time of the superconducting gap [1–3]. Also, pertinently irradiating the system, it is possible to induce the onset of metastable transient states, with peculiar properties, sometimes completely different from the ones of the “true” asymptotic state reached as the time  $t \rightarrow \infty$  [4, 5].

There are at least two main issues that arise in studying the time evolution of nonequilibrium correlated systems. First of all, typically, such systems are characterized by several different phases [6], often close to each other in energy. Knowing their transient dynamics allows for finding out to which phase they flow, once prepared in a given state, thus recovering crucial information about their elementary excitations [7, 8]. Also, controlling their time evolution allows for possibly stabilizing metastable phases, with novel, exotic physical properties, sometimes

rather different from the ones characterizing the equilibrium states [5, 9]. In addition, along their time evolution, it is possible, for the systems, to go through a dynamical phase transition (DPT), driven by the time  $t$ , between the initial state, in which they are prepared at  $t = 0$ , toward the final state, to which they evolve as  $t \rightarrow \infty$  [10–12].

A widely implemented protocol to induce nonequilibrium dynamics in a many-electron system consists in preparing it in the ground state of a specific Hamiltonian, in performing a sudden quench in some parameter(s) of the system Hamiltonian, and eventually in making the system evolve with the final (“after the quench”) Hamiltonian. In the specific case of a superconducting electronic system, the protocol outlined above results in an effective time dependence of the superconducting gap, which can be accounted for by means of a time-dependent generalization of the self-consistent mean-field (SCMF) approach [3, 13].

In this paper, we define and study a procedure for inducing nonequilibrium dynamics in two-dimensional (2D) superconducting systems, involving two, or more than two, components of the order parameter with different symmetry (such as, for instance, an  $s$ -wave and a  $d$ -wave component of the superconducting gap). In analogy to Ref. [3], we set the nonequilibrium dynamics by quenching the interaction strength(s) of the correspond-

ing model Hamiltonian. Eventually, we recover the time-dependent superconducting gap by systematically implementing self-consistency, at any given time  $t > 0$ . In addition, we employ the Lindblad master equation (LME) approach to the dissipative dynamics of the density matrix of the system [14–20], to account for dissipation and damping effects beyond the time-dependent SCMF approximation. Such effects are related to the interaction among quasiparticles, as well as to the coupling between the quasiparticles and the fluctuations of the superconducting order parameter [21]. In fact, we do not derive the LME, rather we consider the most generic equations that can drive the system to thermal equilibrium. As detailed in Ref. [14], this is a standard approach, based on imposing the detailed balance condition and considering all the independent operators defined within the system’s Hilbert space that allow transitions between different system eigenstates.

Within the LME framework, we couple the system to an external bath, able to exchange energy and quasiparticles with the system itself. In doing so, we show how the relaxation dynamics induced by the coupling to the bath naturally drives the superconductor toward its asymptotic, stationary state. We conclude, therefore, that the dissipation works as an effective stabilization mechanism in the time evolution of the system after the quench. Eventually, the mismatch between the phases corresponding to the initial and to the asymptotic state of the superconductor can drive the system across a real-time DPT between the two distinct phases [10–12].

In fact, while the SCMF approach is expected to be unable to capture the complex interplay of nearby phases in strongly correlated superconductors, such as, for instance, cuprates in their underdoped region, it still allows for effectively highlighting the physics of simple models, such as the one we employ here [3]. Moreover, we argue how, resorting to the LME approach, eventually allows for accounting for effects beyond the SCMF approximation, such as the interaction among quasiparticles, as well as the direct coupling between the quasiparticles and the fluctuations of the superconducting order parameter [21].

DPTs typically arise in the time evolution of quantum systems after a parametric quench in the system Hamiltonian [22–29]. In our specific case, in addition to looking at the time dependence of the superconducting order parameter, we approach the DPT by computing the fidelity  $\mathcal{F}(t)$  between the initial state of the system,  $|\psi(0)\rangle$ , and its state at time  $t$ . Indeed, differently from a closed system, where a DPT is typically investigated by looking at the singularities in the Loschmidt echo  $\mathcal{L}(t) = |\langle\psi(0)|\psi(t)\rangle|^2$  [12, 22, 30–33], in open systems the Loschmidt echo (as well as quantities related to it) is no longer applicable to monitor the DPT and it has to be substituted by some more appropriate quantities, such as the fidelity  $\mathcal{F}(t)$  [12, 34].

Although, in this paper, we focus on a limited number of phase transitions, the effectiveness of our method is grounded on its wide applicability to many different

choices for the superconducting gap, such as, for instance, the ones appropriate for 2D oxide superconductors [35–38]. Moreover, by looking at how the time dynamics of the system is affected by the choice of the actual values of the system parameters, we can in principle suggest how to tune the parameters of realistic devices so to realize phases with the desired properties, including a nontrivial topology [39]. Finally, our approach allows, via a synoptic monitoring of the time-dependent superconducting gap, the fidelity, and (in case of a topological DPT, which we address in Ref. [39]) the spin-Hall conductance, for a comprehensive characterization of a DPT.

Our paper is organized as follows:

- In Sec. II, we present our general two-dimensional lattice model Hamiltonian for a planar superconductor, we employ the SCMF approximation to trade it for an effectively quadratic one, we map out the different superconducting phases as a function of the interaction strengths, and we introduce the LME approach to the system coupled to the bath.
- In Sec. III, we discuss in detail the relaxation dynamics of our superconducting system for different choices of the superconducting order parameter before, and after, the sudden change in the interaction strengths.
- In Sec. IV, we compute the fidelity and employ it to characterize a DPT.
- In Sec. V, we discuss and summarize our results and present some possible further extensions of our work.
- In the Appendixes, we present the technical details of our calculations.

## II. MODEL HAMILTONIAN AND METHODS

We now present our lattice model Hamiltonian  $H$  for a planar superconductor.  $H$  encompasses various interaction terms (on-site, nearest-neighbor, next-to-nearest neighbor), allowing for various possible kinds of spin-singlet superconducting order parameters. We then employ the SCMF approximation to recover the phase diagram of  $H$  as a function of the different interaction strengths. Finally, we present the LME approach, which describes the dynamics of the nonequilibrium system coupled to the bath.

### A. Model Hamiltonian for the lattice planar superconductor

Our main model Hamiltonian describes a system of interacting spinful electrons, defined over a 2D square

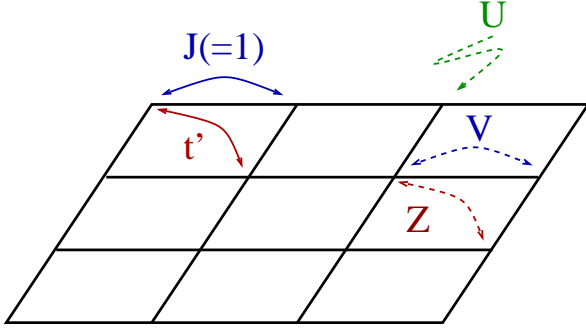


FIG. 1. Sketch of the square lattice with the various single-fermion hopping and interaction terms in Eq.(1): the NN (solid blue) and the NNN (solid red) hopping terms, the on-site (dashed green), the NN (dashed blue), and the NNN (dashed red) interaction terms.

lattice. The single-particle dispersion relation is determined by a nearest-neighbor (NN) hopping strength  $J$  (which we will use as our unit of energy, i.e.,  $J = 1$ ), and a next-to-nearest neighbor (NNN) hopping strength  $t'$ . In addition, we allow for finite on-site, NN and NNN density-density interactions, all in the spin-singlet channel, with interaction strength respectively given by  $U$ ,  $V$  and  $Z$ . Accordingly,  $H$  is given by (see Fig.1)

$$\begin{aligned}
H = & -\mu \sum_{\mathbf{r}} \sum_{\sigma} c_{\mathbf{r},\sigma}^{\dagger} c_{\mathbf{r},\sigma} \\
& - \sum_{\mathbf{r},\hat{\delta}} \sum_{\sigma} c_{\mathbf{r}+\hat{\delta},\sigma}^{\dagger} c_{\mathbf{r},\sigma} - t' \sum_{\mathbf{r},\hat{\delta}'} \sum_{\sigma} c_{\mathbf{r}+\hat{\delta}',\sigma}^{\dagger} c_{\mathbf{r},\sigma} \\
& - U \sum_{\mathbf{r}} n_{\mathbf{r},\uparrow} n_{\mathbf{r},\downarrow} - \frac{V}{2} \sum_{\mathbf{r},\hat{\delta}} n_{\mathbf{r}} n_{\mathbf{r}+\hat{\delta}} - \frac{Z}{2} \sum_{\mathbf{r},\hat{\delta}'} n_{\mathbf{r}} n_{\mathbf{r}+\hat{\delta}'},
\end{aligned} \quad (1)$$

with  $c_{\mathbf{r},\sigma}$ ,  $c_{\mathbf{r},\sigma}^{\dagger}$  being the annihilation and the creation operators for an electron with spin  $\sigma$  at site  $\mathbf{r}$  of a square lattice and  $\mu$  being the chemical potential.  $c_{\mathbf{r},\sigma}$ ,  $c_{\mathbf{r},\sigma}^{\dagger}$  satisfy the canonical anticommutation relations  $\{c_{\mathbf{r},\sigma}, c_{\mathbf{r}',\sigma'}^{\dagger}\} = \delta_{\mathbf{r},\mathbf{r}'} \delta_{\sigma,\sigma'}$ . The spin-polarized density operators in Eq.(1) are defined as  $n_{\mathbf{r},\sigma} = c_{\mathbf{r},\sigma}^{\dagger} c_{\mathbf{r},\sigma}$ , while  $n_{\mathbf{r}} = \sum_{\sigma} n_{\mathbf{r},\sigma}$ . In Eq.(1) we have set the lattice constant to 1.  $\hat{\delta}$  denotes a generic (unit length) vector connecting  $\mathbf{r}$  with the corresponding NN sites of the lattice, while  $\hat{\delta}'$  denotes a generic vector (of length  $\sqrt{2}$ ), connecting  $\mathbf{r}$  with the corresponding NNN sites of the lattice. In the context of solid-state systems, the Hamiltonian  $H$  in Eq.(1) is a generalization of model Hamiltonians widely applied to describe high- $T_c$  superconductors [40–43]. Within alternative platforms, such as cold-atom condensates, optical realizations of systems effectively described by Hamiltonians similar to  $H$  are nowadays within the reach of present technology [44].

In Appendix A, we implement the SCMF approximation to trade  $H$  in Eq.(1) for the corresponding mean-field, quadratic (in the fermionic operators) Hamiltonian  $H_{\text{MF}}$ , given by

$$H_{\text{MF}} = \sum_{\mathbf{k}} \sum_{\sigma} \xi_{\mathbf{k}} c_{\mathbf{k},\sigma}^{\dagger} c_{\mathbf{k},\sigma} - \sum_{\mathbf{k}} \{ \Delta_{\mathbf{k}} c_{\mathbf{k},\uparrow}^{\dagger} c_{-\mathbf{k},\downarrow}^{\dagger} + \text{h.c.} \}, \quad (2)$$

with h.c. standing for Hermitean conjugate and with the single-fermion operators in momentum space,  $c_{\mathbf{k},\sigma}$ , related to the  $c_{\mathbf{r},\sigma}$ 's by means of

$$c_{\mathbf{k},\sigma} = \frac{1}{\sqrt{N}} \sum_{\mathbf{r}} e^{-i\mathbf{k}\cdot\mathbf{r}} c_{\mathbf{r},\sigma}, \quad (3)$$

$N$  being the number of lattice sites. Also, in Eq.(2) we have set

$$\begin{aligned}
\xi_{\mathbf{k}} = & -2[\cos(k_x) + \cos(k_y)] - 4t' \cos(k_x) \cos(k_y) - \mu \\
\Delta_{\mathbf{k}} = & \Delta_S + 2\Delta_{x^2-y^2} \{ \cos(k_x) - \cos(k_y) \} \\
& - 4i\Delta_{xy} \sin(k_x) \sin(k_y), \quad (4)
\end{aligned}$$

with  $\Delta_S$ ,  $\Delta_{x^2-y^2}$ ,  $\Delta_{xy}$  respectively being equal to the s-wave, to the d-wave and to the id-wave components of the superconducting order parameters. As we show in Appendix A, they are determined by the self-consistent equations

$$\begin{aligned}
\Delta_S = & \frac{U}{2N} \sum_{\mathbf{k}} \frac{\Delta_{\mathbf{k}}}{\epsilon_{\mathbf{k}}} \\
\Delta_{x^2-y^2} = & \frac{V}{4N} \sum_{\mathbf{k}} \frac{[\cos(k_x) - \cos(k_y)] \Delta_{\mathbf{k}}}{\epsilon_{\mathbf{k}}} \\
\Delta_{xy} = & \frac{iZ}{2N} \sum_{\mathbf{k}} \frac{\sin(k_x) \sin(k_y) \Delta_{\mathbf{k}}}{\epsilon_{\mathbf{k}}}, \quad (5)
\end{aligned}$$

with the single quasiparticle dispersion relation  $\epsilon_{\mathbf{k}} = \sqrt{\xi_{\mathbf{k}}^2 + |\Delta_{\mathbf{k}}|^2}$ . In the following, when we refer to Eqs.(5) when addressing the system dynamics, we keep  $N$  finite. At variance, to recover the thermodynamics of the system, we refer to the large- $N$  limit of Eqs.(5), in which they become the “standard” integral equations for the superconducting gaps within SCMF approximation, with  $\frac{1}{N} \sum_{\mathbf{k}} \rightarrow \int_{\text{B.Z.}} \frac{d^2k}{(2\pi)^2}$ , with the integral taken over the full Brillouin zone.

At a given  $\mathbf{k}$ , the eigenvalues of  $H_{\text{MF}}$  corresponding to Bogoliubov quasiparticle excitations are given by  $\pm\epsilon_{\mathbf{k}} \equiv \pm\sqrt{\xi_{\mathbf{k}}^2 + |\Delta_{\mathbf{k}}|^2}$ , with the corresponding fermion operator eigenmodes  $\Gamma_{\mathbf{k},\pm}$  determined by the Bogoliubov-Valatin transformation as

$$\begin{bmatrix} \Gamma_{\mathbf{k},+} \\ \Gamma_{\mathbf{k},-} \end{bmatrix} = \begin{bmatrix} \cos\left(\frac{\theta_{\mathbf{k}}}{2}\right) & -e^{i\phi_{\mathbf{k}}} \sin\left(\frac{\theta_{\mathbf{k}}}{2}\right) \\ e^{-i\phi_{\mathbf{k}}} \sin\left(\frac{\theta_{\mathbf{k}}}{2}\right) & \cos\left(\frac{\theta_{\mathbf{k}}}{2}\right) \end{bmatrix} \begin{bmatrix} c_{\mathbf{k},\uparrow} \\ c_{-\mathbf{k},\downarrow}^{\dagger} \end{bmatrix}, \quad (6)$$

and the parameters  $\theta_{\mathbf{k}}$ ,  $\phi_{\mathbf{k}}$  defined by

$$\begin{aligned}
\xi_{\mathbf{k}} = & \epsilon_{\mathbf{k}} \cos(\theta_{\mathbf{k}}) \\
\Delta_{\mathbf{k}} = & \epsilon_{\mathbf{k}} \sin(\theta_{\mathbf{k}}) e^{i\phi_{\mathbf{k}}}. \quad (7)
\end{aligned}$$

We now discuss the various superconducting phases that can set in on varying the parameters of  $H_{\text{MF}}$  and the corresponding phase diagram of the system.

## B. Superconducting phases and phase diagram

In this section, we derive the phase diagram of the system as a function of  $U, V$ , and  $Z$ , by holding  $t'$  and  $\mu$  fixed at selected value(s). To do so, we employ Eqs.(5) to determine  $\Delta_S, \Delta_{x^2-y^2}$ , and  $\Delta_{xy}$  at a given value of the various system parameters.

In particular, we first of all study the phase diagram obtained by setting two of the three interaction strengths to 0 and increasing the third one. In this case, we always find a critical value of the variable interaction strength, beyond which the corresponding superconducting phase sets in. We draw the corresponding phase diagrams in Fig.2, where we plot  $\Delta_S$  as a function of  $U$ , for  $V = Z = 0$  (panel **a**)),  $\Delta_{x^2-y^2}$  as a function of  $V$ , for  $U = Z = 0$  (panel **b**)), and  $\Delta_{xy}$  as a function of  $Z$  for  $U = V = 0$  (panel **c**)), for  $\mu = 0, \mu = 0.8$ , and  $\mu = -0.7$ , respectively, with  $t' = 0$ . In all three cases, we identify the superconducting phase transition, corresponding to the order parameter developing a nonzero value as soon as the corresponding interaction strength becomes greater than a finite critical value. As a function of the chemical potential, the critical value is recovered by solving Eqs.(5) at a given  $\mu$ . In particular, from the plots drawn at different values of  $\mu$ , we see how, as expected [45], the tendency of the system to develop superconducting order is maximal at half-filling ( $\mu = 0$ ), while it gets lower as  $\mu$  is moved to either positive or negative values.

As a next step, we now turn on two different interactions strengths, by holding at zero the third one. In this case, it is possible to recover (at least at SCMF level) phases with two out of  $\Delta_S, \Delta_{x^2-y^2}$  and  $\Delta_{xy}$  being  $\neq 0$ . The importance of phases as such has been, in fact, argued to play a crucial role in the physics of high-temperature superconductors [40, 46–48]. Moreover, the two-gap coexistence can lead to topologically nontrivial superconducting phases, such as the d+id superconductor [49]. Finally, as we discuss in the following, having (at least) two superconducting gaps  $\neq 0$  is an indispensable prerequisite to recover a DPT between superconducting phases (including topologically nontrivial ones), along the time evolution of the nonequilibrium system [38, 39].

As specific model calculations, in Fig.3**a**) we show the phase diagram in the  $U - V$ -plane at  $Z = \mu = t' = 0$ . In this case, from Eqs.(5) we first of all find a normal (N) phase for  $U < U_c$  and  $V < V_c$ , with (for  $\mu = 0$ )  $U_c \approx 0.6$  and  $V_c \approx 0.35$ , and  $\Delta_S = \Delta_{x^2-y^2} = \Delta_{xy} = 0$ . On either increasing  $U$  at fixed (and small)  $V$ , or  $V$  at fixed (and small)  $U$ , we respectively find a purely s-wave superconducting phase with  $\Delta_S \neq 0, \Delta_{x^2-y^2} = \Delta_{xy} = 0$ , and a purely d-wave phase, with  $\Delta_{x^2-y^2} = 0, \Delta_S = \Delta_{xy} = 0$ . For large  $U$  and  $V$  of comparable magnitude, we here find no phase where both  $\Delta_S$  and  $\Delta_{x^2-y^2}$  are  $\neq 0$ . In fact, the system undergoes a direct phase transition from the s-wave to the d-wave superconducting phase (or vice versa). Of course, we note that this is a specific result we obtained within our SCMF approach. While it is unlikely

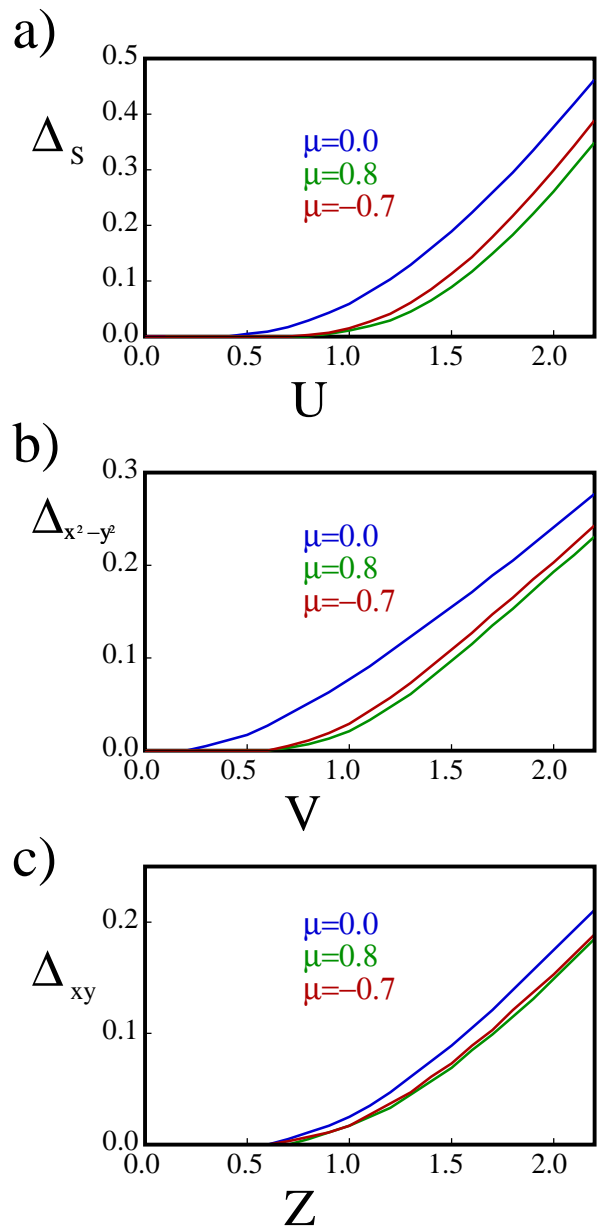


FIG. 2. **a**):  $\Delta_S$  as a function of  $U$  computed from Eqs.(5) by setting  $t' = V = Z = 0$  and  $\mu = 0$  (blue line),  $\mu = 0.8$  (green line) and  $\mu = -0.7$  (red line). **b**):  $\Delta_{x^2-y^2}$  as a function of  $V$  computed from Eqs.(5) by setting  $t' = U = Z = 0$  and  $\mu = 0$  (blue line),  $\mu = 0.8$  (green line) and  $\mu = -0.7$  (red line). **c**):  $\Delta_{xy}$  as a function of  $Z$  computed from Eqs.(5) by setting  $t' = U = V = 0$  and  $\mu = 0$  (blue line),  $\mu = 0.8$  (green line) and  $\mu = -0.7$  (red line).

that a better estimate of the effects of the fluctuations might stabilize a mixed s+d phase, yet, pertinent modifications of our model Hamiltonian (which go beyond the scope of our paper), including additional hoppings and/or interactions, would likely stabilize it.

At variance, as we show in Fig.3**b**), for  $V = 0$ , we find, for  $\mu = 0$ ,  $U_c \approx 0.6$  and  $Z_c \approx 0.7$ . However, in this case, when both  $U$  and  $Z$  are  $\neq 0$  and  $V = 0$ , in

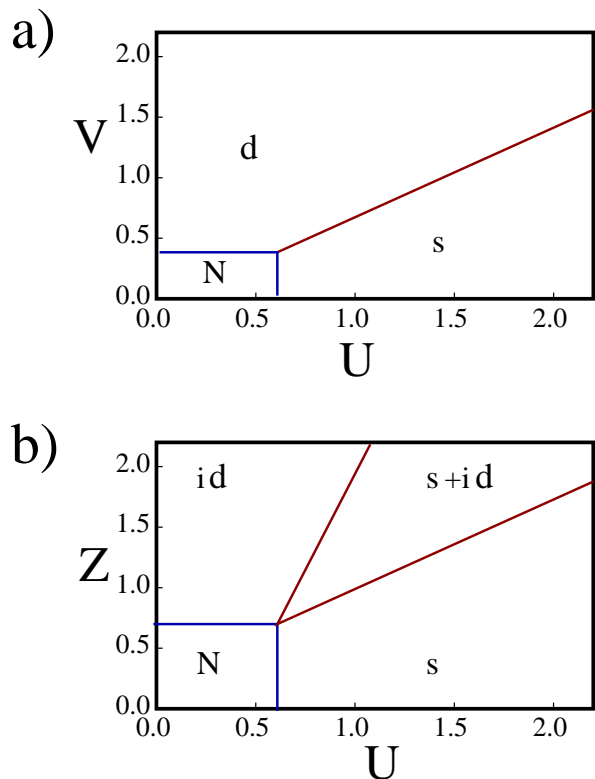


FIG. 3. **a)**: Phase diagram in the  $U - V$  plane computed from Eqs.(5) by setting  $\mu = t' = Z = 0$ . **b)**: Phase diagram in the  $U - Z$  plane computed from Eqs.(5) by setting  $\mu = t' = V = 0$ . In the figure, N,s,d,id, and s+id respectively denote the normal phase (no superconducting gap), an s-wave superconducting phase (only  $\Delta_S \neq 0$ ), a d-wave superconducting phase (only  $\Delta_{x^2-y^2} \neq 0$ ), an id-wave superconducting phase (only  $\Delta_{xy} \neq 0$ ), and the s+id-phase, with both  $\Delta_S$  and  $\Delta_{xy} \neq 0$ .

addition to the “pure”  $s$ -wave and  $id$ -wave phases, we do find a coexistence phase with both  $\Delta_S$  and  $\Delta_{xy} \neq 0$  ( $s + id$ -phase). This is also what happens when  $U = 0$  and both  $V$  and  $Z$  are  $\neq 0$ , where the corresponding  $d + id$ -phase also exhibits nontrivial topological properties [39]. At  $\mu \neq 0$  one finds that, consistently with the results reported in Fig.2, the nonzero chemical potential just determines a mild shrinking of the superconducting regions: a feature that does not substantially affect the main qualitative aspects of the phase diagrams reported in Fig.3.

Finally, we point out that, although, for  $V = Z = 0$  and at half-filling, the superconducting state is degenerate in energy with a charge density wave phase, as soon as a nonzero negative  $V$  and/or  $Z$  is turned on and/or the system is tuned out of half-filling ( $\mu \neq 0$ ), the superconducting phase comes out to be always more stable than the charge density wave one [45]. Consistently with the above conclusion, throughout our paper we focused

onto superconducting phases only, although with different possible kinds of gap order parameter.

Given a phase diagram such as the ones we show in Fig. 3, a protocol leading to a DPT can, in principle, be realized by simply preparing the system in an initial state within a given phase and by quenching, at  $t = 0^+$ , the interaction parameters to a point within a different phase in the phase diagram.

As we evidence above, the real-time evolution induces an effective dependence on time in the superconducting gap order parameter [3]. The time-dependent superconducting gap can be tuned and possibly observed in, e.g., an out-of-equilibrium pump-probe experiment. In such an experiment, the pump pulse induces a change in the gap. At the same time, the reflectivity and the optical conductivity can be measured with a second probe pulse at different pump-probe time delays. The saturated reflectivity and the gap in the real part of the optical conductivity make it possible to monitor the magnitude of the superconducting gap as a function of time [5, 50]. It is also possible to experimentally adjust the interaction strengths  $U, V$ , and  $Z$ , by tuning the electron-phonon coupling like, for example, in synthetic crystals [51], or in time and angle resolved photoemission spectroscopy experiments [52].

### C. Lindblad master equation

We now review the LME approach, which we employ to describe the dynamics of the nonequilibrium open system.

As stated above, our protocol for inducing the relaxation dynamics in the nonequilibrium system consists first in quenching, at  $t = 0$ , the interaction strengths from their initial values  $U^{(0)}, V^{(0)}, Z^{(0)}$  (not necessarily all  $\neq 0$ ), from which we determine the initial state of the system, to  $U^{(1)}, V^{(1)}, Z^{(1)}$ . Along the derivation of Ref.[3], we study the dynamics of our system within a time dependent version of the SCMF approximation, based on the LME approach. This approach recovers the dissipative dynamics induced in the system by the interactions between quasiparticles beyond BCS approximation, and/or by the coupling between the fluctuations of the order parameter and the quasiparticle continuum [21, 25, 53, 54]. Following Refs. [55, 56] and using  $H_{MF}$  in Eq.(2) as our main system Hamiltonian, we write down the full set of LME for the time evolution of the density matrix operator of the system coupled to the bath,  $\rho(t)$ , which we pertinently complement by self-consistently recalculating, at any  $t$ , the (time-dependent) superconducting order parameter  $\Delta_{\mathbf{k}}(t)$ . Eventually, we show that our systematic approach is perfectly consistent with the one introduced in Ref.[21] on phenomenological grounds.

The LME for  $\rho(t)$  has the form

$$\begin{aligned} \frac{d\rho(t)}{dt} = & -i[H_{\text{MF}}(t), \rho(t)] + g \sum_{\lambda=\pm} \sum_{\mathbf{k}} (1 - f(\lambda\epsilon_{\mathbf{k}}(t))) \{[\Gamma_{\mathbf{k},\lambda}(t), \rho(t)\Gamma_{\mathbf{k},\lambda}^\dagger(t)] - [\Gamma_{\mathbf{k},\lambda}^\dagger(t), \Gamma_{\mathbf{k},\lambda}(t)\rho(t)]\} \\ & + g \sum_{\lambda=\pm} \sum_{\mathbf{k}} f(\lambda\epsilon_{\mathbf{k}}(t)) \{[\Gamma_{\mathbf{k},\lambda}^\dagger(t), \rho(t)\Gamma_{\mathbf{k},\lambda}(t)] - [\Gamma_{\mathbf{k},\lambda}(t), \Gamma_{\mathbf{k},\lambda}^\dagger(t)\rho(t)]\} . \end{aligned} \quad (8)$$

In Eq.(8) we have denoted with  $g$  the strength of the coupling between the system and the external bath. Moreover, we have set the coupling strength corresponding to the quasiparticle annihilation and creation operators,  $\Gamma_{\mathbf{k},\lambda}$  and  $\Gamma_{\mathbf{k},\lambda}^\dagger$  (see Eq.(6)), so to make them proportional to  $(1 - f(\lambda\epsilon_{\mathbf{k}}))$  and  $f(\lambda\epsilon_{\mathbf{k}})$ , respectively, with  $f(\epsilon)$  being the Fermi distribution function. Accordingly, Eq.(8) describes the system coupled to a bath with which it can exchange both energy and matter, through the injection or the annihilation of Bogoliubov quasiparticles. Indeed, Lindblad jump operators describe the creation/annihilation of these quasiparticles with, as stated above, a transition probability chosen so to satisfy the detailed balance condition and to make the stationary state of the LME to be described by a thermal grand-canonical density matrix. Our choice is a particular case of the generic system-bath Hamiltonian [as shown in Eq. (3.128) of Ref. [14]], which is realized as a pertinent linear combination of the tensor products between system and bath eigenstates [note that changing the linear combination would only affect the numerical values of the coupling strengths, not the general form, of Eq. (8)].

While, in principle, we could arbitrarily choose the Lindblad jump operators and the corresponding coupling strengths, setting them as we do here, we make sure that the detailed balance is ensured and the Boltzmann distribution is a stationary solution of the Lindblad equation [14, 16]. Moreover, as we discuss below, our choice eventually yields results for the time evolution and for the asymptotic alternative states of our system that are perfectly consistent with the phenomenological approach of Ref. [21]. Since we self-consistently compute the superconducting order parameter,  $\Delta_{\mathbf{k}}(t)$ , at any time  $t$ ,  $H_{\text{MF}}(t)$  at the right-hand side of Eq.(8) acquires an explicit dependence on  $t$  and, accordingly, its eigenvalues  $[\pm\epsilon_{\mathbf{k}}(t)]$  and the corresponding eigenmodes  $[\Gamma_{\mathbf{k},\pm}(t)]$  depend on  $t$ , as well.

To write the SCMF equation for  $\Delta_{\mathbf{k}}(t)$ , we take advantage of the fact that  $H_{\text{MF}}(t)$  is quadratic in the quasiparticle operators and that the coupling to the external bath is linear in the same operators. This allows us to employ Eq. (8) to write a closed set of equations for the (time-dependent) average values of the products of two single-fermion operators. Specifically, we set

$$\begin{aligned} \nu_{\mathbf{k},\sigma}(t) &= \sigma \text{Tr} \left[ \rho(t) \left( c_{\mathbf{k},\sigma}^\dagger c_{\mathbf{k},\sigma} - \frac{1}{2} \right) \right], \\ f_{\mathbf{k}}(t) &= \text{Tr}[\rho(t)c_{\mathbf{k},\downarrow}c_{-\mathbf{k},\uparrow}] . \end{aligned} \quad (9)$$

We now point out that, on one hand, there is zero spin polarization in the initial state, on the other hand, no

spin polarization can either be generated along the dynamical evolution of the system, as described by Eq.(8). Indeed, this can be readily verified by introducing the total spin operator  $\mathbf{S} = \sum_{\mathbf{k}} \mathbf{S}_{\mathbf{k}}$ , with the Anderson isospin operator at given  $\mathbf{k}$ ,  $\mathbf{S}_{\mathbf{k}}$ , defined as.

$$S_{\mathbf{k}}^a = \frac{1}{2} [c_{\mathbf{k},\uparrow}^\dagger, c_{-\mathbf{k},\downarrow}] \sigma^a \begin{bmatrix} c_{\mathbf{k},\uparrow} \\ c_{-\mathbf{k},\downarrow}^\dagger \end{bmatrix} , \quad (10)$$

$\{\sigma^a\}$  being the Pauli matrices. At time  $t$ , we obtain  $\langle \mathbf{S}(t) \rangle = \text{Tr}[\rho(t)\mathbf{S}]$ . From Eq.(8), taking into account that  $[H_{\text{MF}}(t), \mathbf{S}] = 0$  and that the quasiparticle operators  $\Gamma_{\mathbf{k},\lambda}(t)$  carry a well-defined spin content, it can be readily shown that  $\frac{d\langle \mathbf{S}(t) \rangle}{dt} = 0$ , which implies  $\nu_{\mathbf{k},\uparrow}(t) = -\nu_{\mathbf{k},\downarrow}(t) \equiv \nu_{\mathbf{k}}(t)$ . As a result, we recover, in the zero-temperature limit, the (closed) set of differential equations

$$\begin{aligned} \frac{d\nu_{\mathbf{k}}(t)}{dt} &= -\frac{g\xi_{\mathbf{k}}}{\epsilon_{\mathbf{k}}(t)} - 2g\nu_{\mathbf{k}}(t) + \Im m\{[\Delta_{\mathbf{k}}(t)]^* f_{\mathbf{k}}(t)\} \\ \frac{df_{\mathbf{k}}(t)}{dt} &= -(2i\xi_{\mathbf{k}} + 2g)f_{\mathbf{k}}(t) - 2i\Delta_{\mathbf{k}}(t)\nu_{\mathbf{k}}(t) + \frac{g\Delta_{\mathbf{k}}(t)}{\epsilon_{\mathbf{k}}(t)} , \end{aligned} \quad (11)$$

with  $\epsilon_{\mathbf{k}}(t) = \sqrt{\xi_{\mathbf{k}}^2 + |\Delta_{\mathbf{k}}(t)|^2}$  and  $\Im m$  denoting the imaginary part. To compute  $\Delta_{\mathbf{k}}(t)$  we resort to the time-dependent SCMF approach. This corresponds to a time-dependent generalization of the BCS variational ansatz, which is equivalent to assuming a time dependent generalization of the latter one of Eqs.(4) in the form

$$\begin{aligned} \Delta_{\mathbf{k}}(t) &= \Delta_S(t) + 2\Delta_{x^2-y^2}(t)\{\cos(k_x) - \cos(k_y)\} \\ &\quad - 4i\Delta_{xy}(t)\sin(k_x)\sin(k_y) . \end{aligned} \quad (12)$$

The parameters  $\Delta_S(t)$ ,  $\Delta_{x^2-y^2}(t)$ , and  $\Delta_{xy}(t)$  have to be self-consistently computed by employing a pertinent, time-dependent, generalization of Eqs.(5) by replacing  $\Delta_{\mathbf{k}}/\epsilon_{\mathbf{k}}$  at the right-hand side of the equations with  $f_{\mathbf{k}}(t)$  obtained by solving Eqs.(11).

To further ground the time-dependent SCMF approach leading to Eq.(12), we note that the same results as the ones recovered within our approach were derived in Ref.[3] within Keldysh nonequilibrium approach, in the limit of a small change in the interaction strengths.

As we pointed out above, differently from the derivation of Ref.[3], in our approach, the direct coupling to the external bath always determines a finite relaxation timescale ( $\sim (2g)^{-1}$ ) for the superconducting order parameter. This uniquely sets the asymptotic value of  $\Delta_{\mathbf{k}}(t)$  as  $t \rightarrow \infty$  to the one corresponding to the equilibrium superconducting phase described by  $H$  in Eq.(1) with interaction strengths  $U^{(1)}, V^{(1)}, Z^{(1)}$ . As we discuss

in the following, when taking the system across a DPT, the coupling to the external bath is also crucial in setting the time  $t_*$  at which the transition takes place.

In order to physically ground our choice for the Lindblad operators entering the LME in Eq.(8), we now compare our formalism with the phenomenological approach of Ref.[21] (to which we refer for a systematic discussion about the relation between the terms of the phenomenological equation – and, therefore, of the LME – and the microscopic quasiparticle dynamics). To do so, we employ Eqs.(11) (which are a direct consequence of the LME in Eq.(8)) we can, therefore, write down the equations of motion for  $\mathbf{S}_{\mathbf{k}}(t)$  in Eq.(10) as

$$\frac{d\langle \mathbf{S}_{\mathbf{k}}(t) \rangle}{dt} = \langle \mathbf{S}_{\mathbf{k}}(t) \rangle \times \mathbf{B}_{\mathbf{k}}(t) - 2g\langle \mathbf{S}_{\mathbf{k}}(t) \rangle + 2g\langle \mathbf{S}_{\mathbf{k},*}(t) \rangle \quad , \quad (13)$$

with

$$\mathbf{B}_{\mathbf{k}}(t) = \begin{bmatrix} \Re[-\Delta_{\mathbf{k}}(t)] \\ \Im[\Delta_{\mathbf{k}}(t)] \\ \xi_{\mathbf{k}} \end{bmatrix} \quad , \quad (14)$$

and

$$\langle \mathbf{S}_{\mathbf{k},*}(t) \rangle = \frac{1}{2\epsilon_{\mathbf{k}}(t)} \mathbf{B}_{\mathbf{k}}(t) \quad . \quad (15)$$

From Eq.(15) we infer that the vector  $\langle \mathbf{S}_{\mathbf{k},*}(t) \rangle$  is always proportional to  $\mathbf{B}_{\mathbf{k}}(t)$ , that is, fully longitudinal. Thus, we conclude that Eq.(14) has exactly the same form as Eq.(9) of Ref.[21], provided, in the formalism of that paper, one takes the longitudinal ( $T_1^{-1}$ ) and transverse ( $T_2^{-1}$ ) relaxation rates for  $\mathbf{S}_{\mathbf{k}}$  according to  $T_1^{-1} = T_2^{-1} = 2g$ . In fact, finite values of  $T_1^{-1}$  and  $T_2^{-1}$  in a nonequilibrium superconductor have been argued to be related to the (inverse) timescales of integrability-breaking (that is, non BCS-like) interactions. Specifically,  $T_1$  is related to the interaction among quasiparticles, while  $T_2$  to the direct coupling between the quasiparticles and the fluctuations of the superconducting order parameter [21]. In general, both  $T_1$  and  $T_2$  must be regarded as phenomenological parameters, and their values depend on the specific material and on the protocol implemented in the measurement. For instance, in the case in which nonequilibrium is induced by acting with strong optical pulses with Terahertz frequencies on NbN, or on Nb<sub>3</sub>Sn, typical values of the order of 10 ps have been fitted from the experiments discussed in Ref.[21], with a pulse duration of a few ps. Assuming, in our model, an over-all energy scale  $J \sim 1\text{eV}$  would yield  $g \sim 0.002$ . However, since, within our protocol, we assume that the superconductor is adiabatically prepared in the nonequilibrium state, starting from  $t \rightarrow -\infty$ , we may expect, in a realistic system, values of  $g$  that are significantly larger than the previous estimate. Consistently with the uncertainty on its actual value in a realistic system, we perform our calculations for at least two values of  $g$ , typically different by orders of magnitude from each other.

In both cases the bath is a gas of Bogoliubov quasiparticles. In the self-consistent time evolution, the bath is intrinsic to the system and the LME accounts for residual interactions between the Bogoliubov quasiparticles neglected in the mean-field BCS approach [21]; in the non self-consistent time evolution the proximity effect may allow, for instance, for quasiparticles to be exchanged between the system and an underneath superconductor at equilibrium [57].

In the following, we present and discuss our results for the time evolution of the superconducting order parameter in the system coupled to the external bath in some paradigmatic cases. Also, in Appendix B we review the same calculation for the case in which, at  $t = 0$ , one directly quenches  $\Delta_{\mathbf{k}}(t)$ . Besides being useful for comparison with the case in which one quenches the interaction strengths, this latter approach is of great relevance in our calculation of the spin-Hall conductance in Ref.[39].

### III. TIME EVOLUTION OF THE SUPERCONDUCTOR COUPLED TO THE EXTERNAL BATH

We now discuss the time evolution of our nonequilibrium open system. Specifically, we initialize the system in the groundstate of  $H_{\text{MF}}$  with an assigned value of the gap parameter  $\Delta_{\mathbf{k}}^{(0)}$ , corresponding to the state realized at different values of the interaction strengths,  $U^{(0)}$ ,  $V^{(0)}$ , and  $Z^{(0)}$ . Then, at  $t = 0^+$ , we quench the interaction strengths to  $U^{(1)}$ ,  $V^{(1)}$ , and  $Z^{(1)}$  and, at the same time, we turn on the coupling  $g$  to the bath. For  $t > 0$  the system evolves toward its asymptotic state, and the superconducting gaps explicitly depend on  $t$  according to Eqs.(12).

Along our analysis, we first consider the case in which only one of the three interaction strengths is  $\neq 0$  and, at a second stage, we generalize our derivation to the case in which two interaction strengths become  $\neq 0$ . This eventually allows us to investigate whether a DPT is expected to set in along the time evolution of the system and, if so, what are its main features.

Throughout our derivation we work in the zero-temperature limit. In this limit, the function  $f(\lambda\epsilon_{\mathbf{k}}(t))$  in the coupling strengths in front of the Lindblad operators in Eq.(8) is either equal to 0, if  $\lambda = +1$ , or to 1, if  $\lambda = -1$ , regardless of  $t$ . While this provides a remarkable simplification of our derivation below, yet, following our above analysis, it is in principle straightforward to address the finite temperature case as well.

#### A. Relaxation dynamics of a single-component order parameter

We begin by keeping only one among the interaction strengths  $U$ ,  $V$  and  $Z$  to be  $\neq 0$ .

In Fig.4 we plot the superconducting gap, normalized to its asymptotic (that is,  $t \rightarrow \infty$ ) value, for the case in which  $\Delta_S(t) \neq 0$  and  $\Delta_{x^2-y^2}(t) = \Delta_{xy}(t) = 0$  (red curves), in which  $\Delta_{x^2-y^2}(t) \neq 0$  and  $\Delta_S(t) = \Delta_{xy}(t) = 0$  (blue curves), and for the case in which  $\Delta_{xy}(t) \neq 0$  and  $\Delta_{x^2-y^2}(t) = \Delta_S(t) = 0$  (green curves). We respectively set  $g = 0.01$  (Fig.4a), and  $g = 0.05$  (Fig.4b). Here, as basically anywhere else below, we set  $t' = \mu = 0$ . From Fig.4, we see that, for any one of the three gaps, the relaxation rate is solely determined by the coupling to the bath: the larger is  $g$ , the faster is the relaxation of the superconducting order parameter toward its asymptotic value. In addition, we also note a remarkable dependence of the relaxation time on the symmetry of the order parameter. This is demonstrated by the different shape of the curves for different gaps, which is apparent in both cases, although it is much more evident in Fig.4a) due to the smaller value of  $g$  and to the correspondingly slower relaxation of the superconducting gaps. Remarkably, a similar effect also appears for a closed system ( $g = 0$ ) [3]. It is likely related to different dissipation mechanisms that set in along the relaxation of the order parameter. Such effects are, in general, well-captured by the time-dependent SCMF approach. At variance, if one gives up self-consistency and simply “quenches” the superconducting gap at  $t = 0$  (see Appendix B for details), any dependence on the symmetry of the superconducting order parameter is washed out. To evidence this point, in Fig.5, we draw plots similar to the ones in Fig.4 but by giving up self-consistency. Indeed, we then see no appreciable dependence of the time dependent superconducting order parameter on its symmetry.

Another remarkable feature of the time evolution of  $\Delta_{\mathbf{k}}(t)$  is given by the oscillations in the amplitude of the superconducting order parameter. While they have been already noticed and discussed in Ref.[3], in our specific case they exhibit a peculiar behavior, due to the nonzero coupling to the bath. As the system is prepared in a nonequilibrium state that, in principle, has a nonzero overlap with all the excited states of the Hamiltonian that determines the time evolution for  $t > 0$ , we expect, for small time intervals, oscillations in the amplitude of the order parameters over several frequencies. To evidence that this is, in fact, the case, in the inset of Fig.4a) we show the same plot as in the main figure, but restricted to the interval  $0 \leq t \leq 20$ . We clearly see the expected oscillations which, as  $t$  gets large, start to be damped by the finite value of  $g$ . A similar effect can be identified in the inset of Fig.4b), although now the damping is much faster, due to the larger value of  $g$ .

### B. Relaxation dynamics of a two-component order parameter

We now consider the case in which (at least) two interaction strengths are  $\neq 0$ .

We now consider the relaxation dynamics of a system

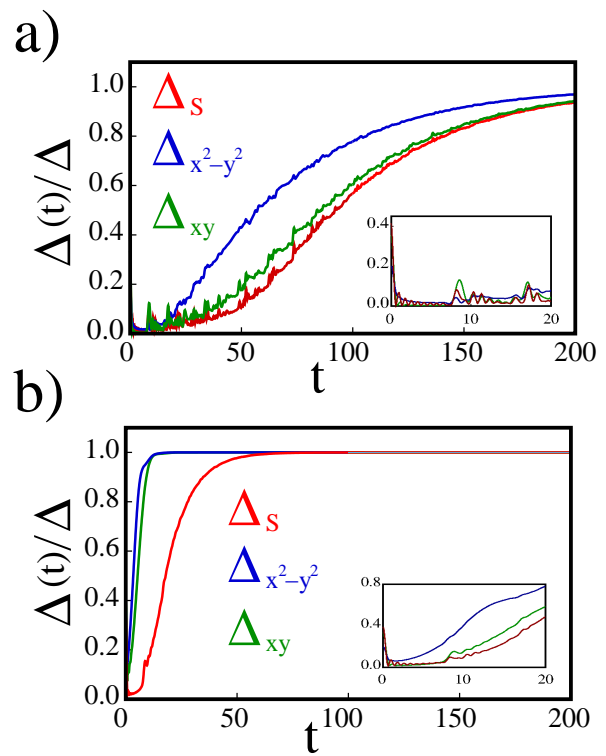


FIG. 4. **a)**: Time evolution of the rescaled order parameters  $\Delta(t)/\Delta$  self-consistently computed for  $g = 0.01$ , for the case in which  $\Delta_S(t=0) = 0.0750$  and  $\Delta_{x^2-y^2}(t=0) = \Delta_{xy}(t=0) = 0$  (computed at  $U = 1.5, V = Z = 0$  – red curves), for the case in which  $\Delta_{x^2-y^2}(t=0) = 0.0607$  and  $\Delta_S(t=0) = \Delta_{xy}(t=0) = 0$  (computed at  $V = 1.5, U = Z = 0$  – blue curves), and for the case in which  $\Delta_{xy}(t=0) = 0.1208$  and  $\Delta_{x^2-y^2}(t=0) = \Delta_S(t=0) = 0$  (computed at  $Z = 1.5, U = V = 0$  – green curves) [Inset: zoom of the plots restricted to the interval  $0 \leq t \leq 20$ ]. **b)**: Same as in panel **a)**, but with  $g = 0.05$ .

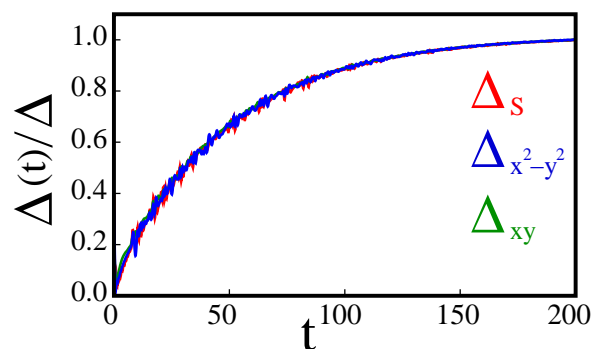


FIG. 5. Time evolution of the rescaled order parameters  $\Delta(t)/\Delta$  non self-consistently computed for  $g = 0.01$ , for the case in which  $\Delta_S(t=0) = 0.075$  and  $\Delta_{x^2-y^2}(t) = \Delta_{xy}(t) = 0$  (computed at  $U = 1.5, V = Z = 0$  – red curve), for the case in which  $\Delta_{x^2-y^2}(t=0) = 0.030$  and  $\Delta_S(t) = \Delta_{xy}(t) = 0$  (computed at  $V = 1.5, U = Z = 0$  – blue curve), and for the case in which  $\Delta_{xy}(t=0) = 0.0302$  and  $\Delta_{x^2-y^2}(t) = \Delta_S(t) = 0$  (computed at  $Z = 1.5, U = V = 0$  – green curve).



prepared in the ground state of  $H_{\text{MF}}$  in Eq.(2), with  $\Delta_S^{(0)} = \Delta_{x^2-y^2}^{(0)} = 0$ , and  $\Delta_{xy}^{(0)} = 0.03$ , which corresponds to having  $U^{(0)} = V^{(0)} = 0$ ,  $Z^{(0)} > 0$ . Moving across  $t = 0$ , we quench the interaction strengths to  $(U^{(1)}, V^{(1)}, Z^{(1)}) = (1.5, 0, 1.5)$ . As a result, the system develops a nonzero  $\Delta_S(t)$  and  $\Delta_{xy}(t)$ , which we compute for two different values of  $g$  and for  $t' = \mu = 0$ .

In Fig.6 we plot  $\Delta_S(t)$  and  $\Delta_{xy}(t)$ . To evidence the effects of the coupling to the bath on the time evolution of the superconducting gap, we perform the calculation for  $g = 0.2$  (Fig.6a) and for  $g = 0.002$  (Fig.6b). We see that, on one hand, there is, for the larger values of  $g$ , a suppression of the oscillations in the superconducting gap. However, in both cases we identify a finite interval of time  $[0, t_*]$  within which  $\Delta_S(t)$  remains pinned at 0 and  $\Delta_{xy}(t)$  keeps finite and basically constant at large  $g$ , while it smoothly increases, with a fast oscillating modulation, at small  $g$ . Also, we note how the ‘‘critical time’’  $t_*$  increases upon lowering  $g$ . As  $t$  goes across  $t_*$ ,  $\Delta_S(t)$  jumps to a finite value. For  $t > t_*$ , for  $g = 0.2$ ,  $\Delta_S(t)$  has a finite value, roughly constant. For  $g = 0.002$ ,  $\Delta_S(t)$  displays damped oscillations. In both cases, however, we clearly see how, as  $t \rightarrow \infty$ ,  $\Delta_S(t)$  converges toward the value  $\Delta_{S,\infty} = 0.15$ . A similar trend is shown by  $\Delta_{xy}(t)$ , for  $t > t_*$  which also asymptotically flows to  $\Delta_{xy,\infty} = 0.073$ . Remarkably,  $(\Delta_S, \Delta_{xy}) = (\Delta_{S,\infty}, \Delta_{xy,\infty}) = (0.15, 0.073)$  is exactly the set of values of the superconducting gap that one finds from in the phase diagram of Fig.3b) for  $U = Z = 1.5$ . Thus, we conclude that the net effect of coupling the system to the bath is to trigger a time evolution of the superconductor between two equilibrium phases, an initial phase with  $\Delta_S^{(0)} = \Delta_{x^2-y^2}^{(0)} = 0$ ,  $\Delta_{xy}^{(0)} = 0.03$ , and a final (asymptotic) phase with  $\Delta_{S,\infty} = 0.15$ ,  $\Delta_{x^2-y^2}^{(1)} = 0$ , and  $\Delta_{xy,\infty} = 0.073$ . Therefore, as a matter of fact, both plots in Fig.6 evidence a DPT in our system, whose precise location ( $t = t_*$ ) does depend on the value of  $g$ . In the following, we further corroborate our conclusion by studying the time dependence of the fidelity between the initial state of the system and the state that, at time  $t$ , is described by the density matrix  $\rho(t)$  [10–12].

To summarize, from the time dependence of the superconducting order parameters, we clearly find evidence for DPTs, basically determined by the mismatch between the initial and the final state of the system. To better ground our conclusions, in the following we estimate the fidelity  $\mathcal{F}(t)$  along the time evolution, finding an excellent consistency with the conclusions about the DPT we recovered from the time-dependent superconducting order parameters.

#### IV. FIDELITY ACROSS THE DYNAMICAL PHASE TRANSITION

In Section III B we inferred the emergence of the DPT from the time dependence of the superconducting order

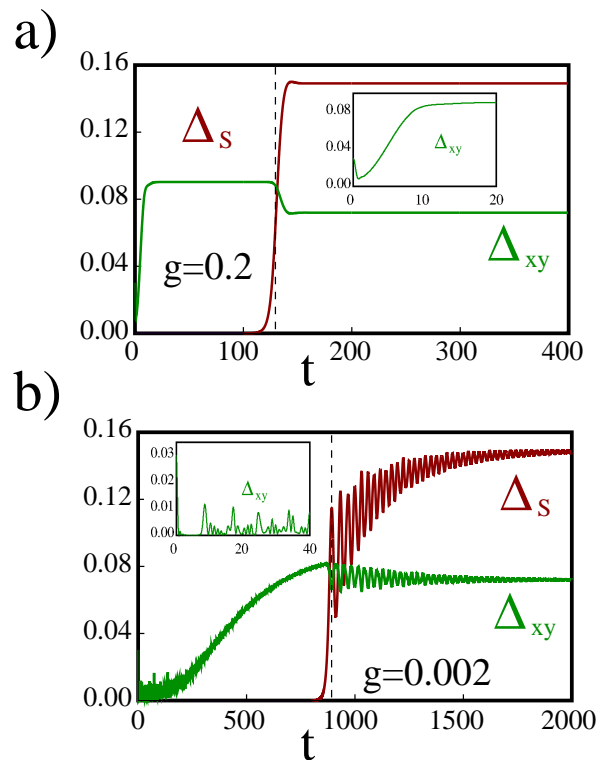


FIG. 6. **a)**: Time evolution of  $\Delta_S(t)$  (red curve) and of  $\Delta_{xy}(t)$  (green curve) computed in a system with  $U = Z = 1.5$ ,  $V = 0$ , coupled to a bath with interaction strength  $g = 0.2$  and prepared, at  $t = 0$ , in a state with  $\Delta_{xy}^{(0)} \approx 0.03$  [Inset: The same plot (for  $\Delta_{xy}(t)$  only), restricted to  $0 \leq t < 20$ ]. **b)**: Same as in panel **a)** but with  $g = 0.002$ . In both cases the vertical dashed lines mark the onset of the DPT [Inset: The same plot (for  $\Delta_{xy}(t)$  only), restricted to  $0 \leq t < 40$ ].

parameter after quenching the interaction strengths. In general, in a closed nonequilibrium system that, at time  $t$ , is described by a pure state  $|\psi(t)\rangle$ , the standard mean to analyze a DPT is looking at nonanalyticities in the Loschmidt echo  $\mathcal{L}(t) = |\langle \psi(0) | \psi(t) \rangle|^2$ , with  $|\psi(0)\rangle$  being the initial state of the system [10–12]. In our case, for  $t > 0$ , the state is described by the density matrix  $\rho(t)$  which, in general, does not correspond to a pure quantum state. For this reason, we now characterize the DPT by looking at nonanalyticities in the fidelity  $\mathcal{F}(t)$  between  $|\psi(0)\rangle$  and density matrix  $\rho(t)$  [10–12, 34]. Specifically, in our case  $\mathcal{F}(t)$  is defined as [58]

$$\mathcal{F}(t) = \langle \psi(0) | \rho(t) | \psi(0) \rangle \quad . \quad (16)$$

The time evolution of  $\rho(t)$  for  $t > 0$  is determined according to the LME in Eq.(8). Due to the time-dependent self-consistency, Eq.(8) is effectively nonlinear and, therefore, it is quite a formidable task to solve it in practice, even for small lattices. For this reason, in the following we resort to a sequence of reasonable approximations, which eventually allow us to recast  $\mathcal{F}(t)$  in a tractable form.

To begin with, let us introduce the basis of the  $\mathcal{N}$ -

particle many-body states created by the quasiparticle creation operators determined by  $H_{\text{MF}}(t)$ . Specifically, we set

$$|\mathcal{N}, t\rangle_{\{\mathbf{q}_j\}, \{\lambda_j\}} = \prod_{j=1}^{\mathcal{N}} [\Gamma_{\mathbf{q}_j, \lambda_j}(t)]^\dagger |\mathbf{0}\rangle, \quad (17)$$

with the vacuum  $|\mathbf{0}\rangle$  defined by the condition  $\Gamma_{\mathbf{q}, \lambda}(t)|\mathbf{0}\rangle = 0$ ,  $\forall \mathbf{q}, \lambda$ . Now, on numerically integrating

$$\begin{aligned} \frac{\partial \rho(t)}{\partial t} \approx & -i\{H_{\text{MF}}(t)\rho(t) - \rho(t)H_{\text{MF}}(t)\} - g \sum_{\mathbf{k}} \{[\Gamma_{\mathbf{k},+}(t)]^\dagger \Gamma_{\mathbf{k},+}(t)\rho(t) \\ & + \rho(t)[\Gamma_{\mathbf{k},+}(t)]^\dagger \Gamma_{\mathbf{k},+}(t) + \Gamma_{\mathbf{k},-}(t)[\Gamma_{\mathbf{k},-}(t)]^\dagger \rho(t) + \rho(t)\Gamma_{\mathbf{k},-}(t)[\Gamma_{\mathbf{k},-}(t)]^\dagger\} \quad . \end{aligned} \quad (18)$$

As a result, retaining only the matrix elements of  $\rho(t)$  between states at half-filling (that is, states containing  $\mathcal{N} = N$  particles, due to the spin degeneracy), we write it in the approximate form

$$\begin{aligned} \rho(t) \approx & \sum_{\{\mathbf{q}_j\}} \sum_{\{\lambda_j\}; \{\mu_j\}} \rho_{\{\lambda_j\}, \{\mu_j\}, \{\mathbf{q}_j\}}^{(N)}(t) \times \\ & |N, t\rangle_{\{\mathbf{q}_j\}, \{\lambda_j\}} \langle N, t|_{\{\mathbf{q}_j\}, \{\mu_j\}}, \end{aligned} \quad (19)$$

with  $N$  being the number of lattice sites.

Next, we note that, due to the parametric dependence on  $t$  of the operators  $\Gamma_{\mathbf{k}, \lambda}(t)$ , a solution of the time-dependent Schrödinger equation

$$\frac{\partial}{\partial t} |\psi(t)\rangle = H_{\text{MF}}(t)|\psi(t)\rangle, \quad (20)$$

is not simply provided by setting

$$|\psi(t)\rangle = \exp \left[ -i \int_0^t \sum_{j=1}^N \lambda_j \epsilon_{\mathbf{q}_j}(\tau) d\tau \right] |N, t\rangle_{\{\mathbf{q}_j\}, \{\lambda_j\}}, \quad (21)$$

as one would in fact obtain

$$\begin{aligned} \frac{\partial}{\partial t} |\psi(t)\rangle = & -iH_{\text{MF}}(t)|\psi(t)\rangle + \\ \exp \left[ -i \int_0^t \sum_{j=1}^N \lambda_j \epsilon_{\mathbf{q}_j}(\tau) d\tau \right] & \frac{\partial}{\partial t} |N, t\rangle_{\{\mathbf{q}_j\}, \{\lambda_j\}}. \end{aligned} \quad (22)$$

Yet, while the ‘‘dynamical’’ phases at the right-hand side of Eq.(21) typically grow linearly with time  $t$ , the time evolution of the state  $|N, t\rangle_{\{\mathbf{q}_j\}, \{\lambda_j\}}$  (which is determined by the parametric dependence on  $t$  of the operators  $\Gamma_{\mathbf{k}, \lambda}(t)$ ), takes place over periodic patterns in time. For this reason, it is reasonable to assume that the dependence on time of the dynamical phases takes place over typical frequencies much larger than the one associated to the parametric dependence of  $|N, t\rangle_{\{\mathbf{q}_j\}, \{\lambda_j\}}$  on  $t$ . Thus, in the following we neglect the latter contribution

Eqs.(11) for  $\nu_{\mathbf{k}}(t)$ , we easily verify that, in the half-filled system,  $\nu_{\mathbf{k}}(t) = 0$  constantly, along the time evolution. Therefore, consistently with the result that, on average, we get  $\mathcal{N} = N$ , we make the assumption that all the density matrix elements involving states with total filling different from  $1/2$  are negligible and, then, can be safely put equal to 0. This allows us to simplify the right-hand side of Eq.(8) by neglecting terms that would change  $\mathcal{N}$ . Accordingly, we resort to the approximate equation for  $\rho(t)$  given by

to the right-hand side of Eq.(22). This leads us to write a simplified (and closed) set of equations for the matrix elements  $\rho_{\{\lambda_j\}, \{\mu_j\}, \{\mathbf{q}_j\}}^{(N)}(t)$ , given by

$$\begin{aligned} \frac{\rho_{\{\lambda_j\}, \{\mu_j\}, \{\mathbf{q}_j\}}^{(N)}(t)}{dt} = & \\ -i \sum_{j=1}^N \{ [\lambda_j - \mu_j] \epsilon_{\mathbf{q}_j}(t) \} & \rho_{\{\lambda_j\}, \{\mu_j\}, \{\mathbf{q}_j\}}^{(N)}(t) \\ -g \{ 2N + \sum_{j=1}^N [\lambda_j + \mu_j] \} & \rho_{\{\lambda_j\}, \{\mu_j\}, \{\mathbf{q}_j\}}^{(N)}(t). \end{aligned} \quad (23)$$

Upon integrating Eqs.(23), we obtain

$$\begin{aligned} \rho_{\{\lambda_j\}, \{\mu_j\}, \{\mathbf{q}_j\}}^{(N)}(t) = & e^{[-i \int_0^t d\tau \sum_{j=1}^N [\lambda_j - \mu_j] \epsilon_{\mathbf{q}_j}(\tau)]} \times \\ \exp \left[ -g \left\{ 2N + \sum_{j=1}^N [\lambda_j + \mu_j] \right\} t \right] & \rho_{\{\lambda_j\}, \{\mu_j\}, \{\mathbf{q}_j\}}^{(N)}(0). \end{aligned} \quad (24)$$

An important consequence of Eq.(24) is that all the elements  $\rho_{\{\lambda_j\}, \{\mu_j\}, \{\mathbf{q}_j\}}^{(N)}(t)$  are exponentially suppressed, as soon as  $2gt \geq 1$ , except for the diagonal ones with  $\lambda_1 = \dots = \lambda_N = -$ , and  $\mu_1 = \dots = \mu_N = -$ . Over time scales  $> (2g)^{-1}$ , we therefore obtain

$$\rho(t) \approx |N, t\rangle_{\{\mathbf{q}_j\}, \{-\}} \langle N, t|_{\{\mathbf{q}_j\}, \{-\}}. \quad (25)$$

Moreover, we point out how, in writing the right-hand side of Eq.(25), we did not sum over the  $\mathbf{q}_j$ , as the state  $|N, t\rangle_{\{\mathbf{q}_j\}, \{-\}}$  is uniquely fixed by populating the negative-energy modes at time  $t$  for all possible values of  $\mathbf{q}_j$ . As a result of our approximations, we eventually find

$$\begin{aligned} \mathcal{F}(t) = & \langle \psi(0) | \rho(t) | \psi(0) \rangle \\ \approx & |\langle \psi(0) | N, t\rangle_{\{\mathbf{q}_j\}, \{-\}}|^2. \end{aligned} \quad (26)$$

Remarkably, Eq.(26), which is valid for  $2gt > 1$  and which provides us with the starting point of our following

derivation, coincides with the value that the Loschmidt echo would have in a closed system whose (pure) collective state, at time  $t > 0$ , is given by  $|\psi(t)\rangle = \prod_j [\Gamma_{\mathbf{q}_j, -}(t)]^\dagger |\mathbf{0}\rangle$ . In fact, the analogy is not accidental. For a closed system, the Loschmidt echo is nothing but a fidelity between the state at the initial time  $t = 0$  and its time-evolved counterpart at general  $t$ . Therefore, if the evolved state crosses a quantum phase transition, a nonanalyticity is expected on  $\mathcal{F}(t)$  [12, 59, 60].

To probe the DPT, in the following we rather look for nonanalyticities in the rate function  $\omega(t)$ , defined as [10–12, 23, 39]

$$\omega(t) = -\frac{1}{N} \log[\mathcal{F}(t)] \quad , \quad (27)$$

by computing  $\mathcal{F}(t)$  as

$$\mathcal{F}(t) = |\langle \psi(t=0) | \mathcal{U}(t) | \psi(t=0) \rangle|^2 \quad , \quad (28)$$

with  $\mathcal{U}(t) = \mathcal{T} \exp \left[ -i \int_0^t d\tau H(\tau) \right]$ , where  $\mathcal{T}$  is the time-ordered evolution operator. To compute the right-hand side of Eq.(28), we follow a two-step procedure. Specifically, we first numerically compute  $\Delta_{\mathbf{k}}(t)$  within the time-dependent SCMF approximation. Therefore, we use  $\Delta_{\mathbf{k}}(t)$  self-consistently computed as an input parameter of the time-dependent Hamiltonian  $H_{\text{MF}}(t)$ , which we eventually employ to compute the right-hand side of Eq.(28). In this way, we compute  $\omega(t)$  along the time evolution of the systems with parameters set as in drawing Fig.6. In Fig.7 we draw the corresponding plot of  $\omega(t)$ . The blue and the red curve respectively correspond to  $g = 0.2$  and to  $g = 0.002$ , with all the other parameters chosen exactly as in Fig.6. In both cases we mark with a vertical dashed line the time  $t = t_*$  at which the system goes through the DPT. Despite some differences between the two plots, including, of course, the different values for  $t_*$  determined by the different values of  $g$ , we note an over-all similar behavior of  $\omega(t)$ . Specifically, for  $0 \leq t < t_*$ ,  $\omega(t)$  takes only a mild time dependence on  $t$ , with  $\omega(t) \sim 0.1 - 0.2$ , denoting an appreciable overlap between  $|\psi(0)\rangle$  and  $|\psi(t)\rangle$ . Therefore, we see that the first part of the plots indicate the persistence of the system in the initial pre-quench phase for times  $t$  up to the transition time  $t_*$  [12]. At  $t = t_*$ , a sudden change in the slope of  $\omega(t)$  evidences how  $t = t_*$  corresponds to a point where the derivative of  $\omega(t)$  does not exist, that is, to a typical sort of nonanalyticity that signals a DPT. For  $t > t_*$ , the rapid increase in  $\omega(t)$ , following the sudden change in the slope, corresponds to a drastic reduction in  $\mathcal{F}(t)$  (by orders of magnitude), which is a clear signal that, moving across  $t = t_*$ , the system has gone through a DPT.

About the relation between  $t_*$  and the coupling  $g$  we note that the physical intuition behind the existence of a critical time for a DPT is related to the geometric properties of the energy landscape of the system [61]. During the dissipative dynamics induced by the coupling with the bath, the system evolves with a speed that depends

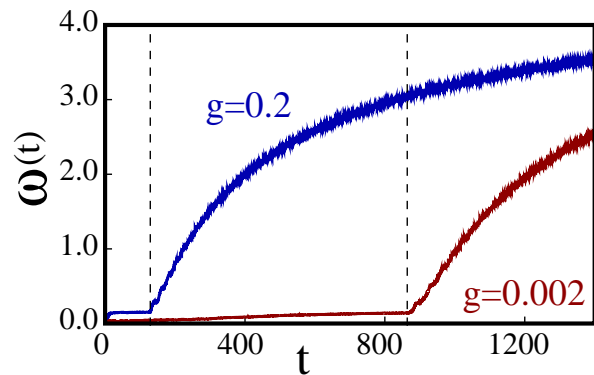


FIG. 7. Rate function  $\omega(t)$  (Eq.(27)) as a function of time  $t$  computed with the time-dependent MF Hamiltonian with parameters  $\Delta_S(t)$  and  $\Delta_{xy}(t)$  as in Fig.6, using  $g = 0.2$  (blue curve) and  $g = 0.002$  (red curve). The dashed vertical lines mark the DPT in the two cases.

on its geometric properties. If the system crosses a “flat” region in energy, the time evolution is extremely slow. As soon as the edge of the stationary solution is reached, the evolution becomes extremely fast and the DPT toward the true stationary solution takes place. The critical time at which this happens depends on the trajectory itself and can not easily be predicted due to the fact that the energy landscape itself is a function of time in the SCMF. A similar behavior has been observed in a much simpler spin system, where it has also been observed that  $t_*$  can depend on the existence of shortcuts in the energy landscapes [16], or on the values of the bath-system coupling strengths [18].

While we do not discuss this point in our paper, it is finally worth mentioning that, in addition to the fidelity, one might also potentially use the entropy  $S(t)$  as an effective mean to detect the DPT. Indeed, along the derivation presented in Ref. [62], we expect that, in the zero-temperature limit,  $S(t)$  for our system would be 0 both at  $t = 0$  (because our system is prepared in a pure state), as well as for  $t \rightarrow \infty$  (because asymptotically our system is described by a Boltzmann distribution at  $T = 0$ ). In between, for  $g = 0.2$ , from the plot of Fig.6a), we infer that the time evolution of the system is characterized by large intervals of time over which the gaps keep constant, and by rapid changes in the gap themselves right after starting the time evolution and at the DPT. The rapid changes in the gaps can be effectively regarded as quenches of the superconducting order parameters. Therefore, by analogy with what is discussed in Ref.[62] for a bosonic system, we expect that a significant number of quasiparticle excitations are created at any change in the gaps, contributing to a corresponding sharp increase of the entropy. The increase of the entropy should, therefore, work as a signal of the DPT. At smaller values of  $g$ , we expect that the entropy increase is present at the DPT, as well, although the feature should be smoother and less marked.

## V. DISCUSSION AND CONCLUSIONS

In this paper we have constructed a protocol to induce nonequilibrium dynamics in an open, superconducting system coupled to an external bath. Pertinently choosing the jump operators in the Lindblad master equation approach to the dissipative dynamics of the density matrix of the system, we let the system evolve toward the thermodynamical stationary state, by making sure that the Boltzmann distribution is a stationary solution of the Lindblad equation. Along our derivation, we have discussed in detail how the mismatch between the initial state and the asymptotic state of the system can lead to a dynamical phase transition, which, under suitable conditions, may also determine a transition between a topologically nontrivial and a topologically trivial phase, or vice versa [39].

To monitor the system across the DPT, we look at the self-consistently computed superconducting gap  $\Delta_{\mathbf{k}}(t)$  and at the fidelity  $\mathcal{F}(t)$ . At the time  $t_*$  at which the phase transition takes place, the components of  $\Delta_{\mathbf{k}}(t)$  abruptly change: this corresponds to a nonanalyticity (a change in the slope) of the function  $\omega(t) = -\frac{\ln \mathcal{F}(t)}{N}$ , that is, a point where  $\omega(t)$  is not differentiable.

As a general comment we note that, while there is already a remarkable amount of results on DPTs in closed systems, still very little is known about DPTs in open systems. In our paper, we attempt to fill such a gap by performing an explicit model calculation of a DPT in superconducting, open systems. Among the results we obtain along our derivation we show how, in an open system, the mismatch between the initial state and the choice of the Hamiltonian parameters, combined with the relaxation dynamics due to the coupling to the bath, triggers the onset of the DPT, how the location in time of the DPT ( $t_*$ ) is affected by the coupling to the bath, and how it is possible, by pertinently tuning the system parameters, to select the asymptotic state toward which the system evolves.

In principle, our approach can be readily generalized to a generic dynamical phase transition in other many-body, fermionic systems [63–65]. Of course, our model is amenable to substantial improvements, possibly on the numerical computational side, such as resorting to a fully time-dependent mean field Hamiltonian  $H_{\text{MF}}(t)$ , in which  $\Delta_{\mathbf{k}}(t)$ , self-consistently computed, should appear as a time-dependent parameter. Also, it would be extremely interesting to perform a systematic analysis of how the critical time  $t_*$  depends on the value of  $g$ , thus to eventually recover the results of Ref. [3] as a limiting case of ours. While interesting, all these tasks fall beyond the scope of this paper, and we are planning to address them as a further development of the work we present here.

**Acknowledgements:** We thank N. Lo Gullo and F. Plastina for insightful discussions. A.N., C.A.P., L.L., and D.G. acknowledge financial support from Italy's

MIUR PRIN project TOP-SPIN (Grant No. PRIN 20177SL7HC). L.L. acknowledges financial support by a project funded under the National Recovery and Resilience Plan (NRRP), Mission 4 Component 2 Investment 1.3 - Call for tender No. 341 of 15/03/2022 of Italian Ministry of University and Research funded by the European Union – NextGenerationEU, award number PE0000023, Concession Decree No. 1564 of 11/10/2022 adopted by the Italian Ministry of University and Research, CUP D93C22000940001, Project title "National Quantum Science and Technology Institute" (NQSTI). A.N. and R.E. acknowledge funding by the Deutsche Forschungsgemeinschaft (DFG, German Research Foundation) under Grant No. 277101999, TRR 183 (project C01), under Germany's Excellence Strategy - Cluster of Excellence Matter and Light for Quantum Computing (ML4Q) EXC 2004/1 - 390534769, and under Grant No. EG 96/13-1.

### Appendix A: Self-consistent mean-field approximation for the superconducting Hamiltonian in Eq.(1)

In this appendix we provide the details of the SCMF approximation, through which we trade  $H$  in Eq.(1) for the MF Hamiltonian,  $H_{\text{MF}}$  in Eq.(2).

In the Hamiltonian of Eq.(1) we have introduced three different interactions, which, in resorting to the SCMF approximation, we decouple as follows:

- *Local superconducting pairing:*

$$\begin{aligned}
 & -U \sum_{\mathbf{r}} \langle c_{\mathbf{r},\uparrow}^\dagger c_{\mathbf{r},\uparrow} c_{\mathbf{r},\downarrow}^\dagger c_{\mathbf{r},\downarrow} \rangle \rightarrow U \sum_{\mathbf{r}} \langle c_{\mathbf{r},\downarrow} c_{\mathbf{r},\uparrow} \rangle \langle c_{\mathbf{r},\uparrow}^\dagger c_{\mathbf{r},\downarrow}^\dagger \rangle \\
 & -U \sum_{\mathbf{r}} \langle c_{\mathbf{r},\downarrow} c_{\mathbf{r},\uparrow} \rangle c_{\mathbf{r},\uparrow}^\dagger c_{\mathbf{r},\downarrow}^\dagger - U \sum_{\mathbf{r}} c_{\mathbf{r},\downarrow} c_{\mathbf{r},\uparrow} \langle c_{\mathbf{r},\uparrow}^\dagger c_{\mathbf{r},\downarrow}^\dagger \rangle = \\
 & \frac{N}{U} |\Delta_S|^2 - \sum_{\mathbf{r}} \{ \Delta_S c_{\mathbf{r},\uparrow}^\dagger c_{\mathbf{r},\downarrow}^\dagger + \Delta_S^* c_{\mathbf{r},\downarrow} c_{\mathbf{r},\uparrow} \} , \quad (\text{A1})
 \end{aligned}$$

with  $\Delta_S = U \langle c_{\mathbf{r},\downarrow} c_{\mathbf{r},\uparrow} \rangle$ .

- *Nearest-neighbor superconducting pairing:*

$$\begin{aligned}
 & -\frac{V}{2} \sum_{\mathbf{r},\hat{\delta}} \sum_{\sigma} \sum_{\sigma'} c_{\mathbf{r},\sigma}^\dagger c_{\mathbf{r},\sigma} c_{\mathbf{r}+\hat{\delta},\sigma'}^\dagger c_{\mathbf{r}+\hat{\delta},\sigma'} \\
 & \rightarrow \frac{V}{2} \sum_{\mathbf{r}} \sum_{\hat{\delta}} \sum_{\sigma} \langle c_{\mathbf{r},\sigma} c_{\mathbf{r}+\hat{\delta},\sigma} \rangle \langle c_{\mathbf{r}+\hat{\delta},\sigma}^\dagger c_{\mathbf{r},\sigma}^\dagger \rangle \\
 & -\frac{V}{2} \sum_{\mathbf{r}} \sum_{\hat{\delta}} \sum_{\sigma} \langle c_{\mathbf{r},\sigma} c_{\mathbf{r}+\hat{\delta},\sigma} \rangle c_{\mathbf{r}+\hat{\delta},\sigma}^\dagger c_{\mathbf{r},\sigma}^\dagger \\
 & -\frac{V}{2} \sum_{\mathbf{r}} \sum_{\hat{\delta}} \sum_{\sigma} c_{\mathbf{r},\sigma} c_{\mathbf{r}+\hat{\delta},\sigma} \langle c_{\mathbf{r}+\hat{\delta},\sigma}^\dagger c_{\mathbf{r},\sigma}^\dagger \rangle = \\
 & \frac{N}{V} \sum_{\hat{\delta}} |\Delta_{NN}(\hat{\delta})|^2 - \sum_{\mathbf{r}} \sum_{\hat{\delta}} \{ \Delta_{NN}(\hat{\delta}) c_{\mathbf{r}+\hat{\delta},\uparrow}^\dagger c_{\mathbf{r},\downarrow}^\dagger \\
 & + [\Delta_{NN}(\hat{\delta})]^* c_{\mathbf{r},\downarrow} c_{\mathbf{r}+\hat{\delta},\uparrow} \} , \quad (\text{A2})
 \end{aligned}$$

with  $\Delta_{NN}(\hat{\delta}) = V\langle c_{\mathbf{r},\downarrow}c_{\mathbf{r}+\hat{\delta},\uparrow} \rangle$  and with the additional assumption that  $\langle c_{\mathbf{r},\downarrow}c_{\mathbf{r}+\hat{\delta},\uparrow} \rangle = -\langle c_{\mathbf{r},\uparrow}c_{\mathbf{r}-\hat{\delta},\downarrow} \rangle$ . (Here,  $\bar{\sigma} = -\sigma$  is the spin index opposite to  $\sigma$ .)

- *Next-to-nearest-neighbor superconducting pairing:*

$$\begin{aligned}
& -\frac{Z}{2} \sum_{\mathbf{r},\hat{\delta}'} \sum_{\sigma} \sum_{\sigma'} c_{\mathbf{r},\sigma}^{\dagger} c_{\mathbf{r},\sigma} c_{\mathbf{r}+\hat{\delta}',\sigma'}^{\dagger} c_{\mathbf{r}+\hat{\delta}',\sigma'} \\
& \rightarrow \frac{Z}{2} \sum_{\mathbf{r}} \sum_{\hat{\delta}'} \sum_{\sigma} \langle c_{\mathbf{r},\sigma} c_{\mathbf{r}+\hat{\delta}',\bar{\sigma}} \rangle \langle c_{\mathbf{r}+\hat{\delta}',\bar{\sigma}}^{\dagger} c_{\mathbf{r},\sigma}^{\dagger} \rangle \\
& -\frac{Z}{2} \sum_{\mathbf{r}} \sum_{\hat{\delta}} \sum_{\sigma} \langle c_{\mathbf{r},\sigma} c_{\mathbf{r}+\hat{\delta},\bar{\sigma}} \rangle c_{\mathbf{r}+\hat{\delta},\bar{\sigma}}^{\dagger} c_{\mathbf{r},\sigma}^{\dagger} \\
& -\frac{Z}{2} \sum_{\mathbf{r}} \sum_{\hat{\delta}} \sum_{\sigma} c_{\mathbf{r},\sigma} c_{\mathbf{r}+\hat{\delta},\bar{\sigma}} \langle c_{\mathbf{r}+\hat{\delta},\bar{\sigma}}^{\dagger} c_{\mathbf{r},\sigma}^{\dagger} \rangle = \\
& \frac{N}{Z} \sum_{\hat{\delta}} |\Delta_{NNN}(\hat{\delta}')|^2 - \sum_{\mathbf{r}} \sum_{\hat{\delta}} \{ \Delta_{NNN}(\hat{\delta}') c_{\mathbf{r}+\hat{\delta},\uparrow}^{\dagger} c_{\mathbf{r},\downarrow}^{\dagger} \\
& + [\Delta_{NNN}(\hat{\delta}')]^* c_{\mathbf{r},\downarrow} c_{\mathbf{r}+\hat{\delta},\uparrow} \} , \quad (\text{A3})
\end{aligned}$$

with  $\Delta_{NNN}(\hat{\delta}') = Z\langle c_{\mathbf{r},\downarrow}c_{\mathbf{r}+\hat{\delta}',\uparrow} \rangle$  and with the additional assumption that  $\langle c_{\mathbf{r},\downarrow}c_{\mathbf{r}+\hat{\delta}',\uparrow} \rangle = -\langle c_{\mathbf{r},\uparrow}c_{\mathbf{r}-\hat{\delta}',\downarrow} \rangle$ .

Resorting to Fourier space, we obtain  $H = H_K + H_P + H_Q$ , with the kinetic energy and the pairing term respectively given by

$$\begin{aligned}
H_K &= \sum_{\mathbf{k}} \sum_{\sigma} \{ -2[\cos(k_x) + \cos(k_y)] - 2t'[\cos(k_x + k_y) + \cos(k_x - k_y)] - \mu \} c_{\mathbf{k},\sigma}^{\dagger} c_{\mathbf{k},\sigma} \equiv \sum_{\mathbf{k}} \sum_{\sigma} \xi_{\mathbf{k}} c_{\mathbf{k},\sigma}^{\dagger} c_{\mathbf{k},\sigma} \\
H_P &= -\sum_{\mathbf{k}} \{ \Delta_S + \sum_{\hat{\delta}} e^{-i\mathbf{k}\cdot\hat{\delta}} \Delta_{NN}(\hat{\delta}) + \sum_{\hat{\delta}'} e^{-i\mathbf{k}\cdot\hat{\delta}'} \Delta_{NNN}(\hat{\delta}') \} c_{\mathbf{k},\uparrow}^{\dagger} c_{-\mathbf{k},\downarrow}^{\dagger} + \text{h.c.} \\
&\equiv -\sum_{\mathbf{k}} \{ \Delta_{\mathbf{k}} c_{\mathbf{k},\uparrow}^{\dagger} c_{-\mathbf{k},\downarrow}^{\dagger} + [\Delta_{\mathbf{k}}]^* c_{-\mathbf{k},\downarrow} c_{\mathbf{k},\uparrow} \} , \quad (\text{A4})
\end{aligned}$$

with

$$\begin{aligned}
\xi_{\mathbf{k}} &= -2[\cos(k_x) + \cos(k_y)] - 4t' \cos(k_x) \cos(k_y) - \mu \\
\Delta_{\mathbf{k}} &= \Delta_S + \sum_{\hat{\delta}} e^{-i\mathbf{k}\cdot\hat{\delta}} \Delta_{NN}(\hat{\delta}) + \sum_{\hat{\delta}'} e^{-i\mathbf{k}\cdot\hat{\delta}'} \Delta_{NNN}(\hat{\delta}') .
\end{aligned}$$

Setting

$$\begin{aligned}
\Delta_{NN}(\hat{\delta}) &= \begin{cases} +\Delta_{x^2-y^2} , & \text{if } \hat{\delta} = \pm\hat{x} \\ -\Delta_{x^2-y^2} , & \text{if } \hat{\delta} = \pm\hat{y} \end{cases} \\
\Delta_{NNN}(\hat{\delta}') &= \begin{cases} -i\Delta_{xy} , & \text{if } \hat{\delta}' = \pm(\hat{x} + \hat{y}) \\ +i\Delta_{xy} , & \text{if } \hat{\delta}' = \pm(\hat{x} - \hat{y}) \end{cases} , \quad (\text{A5})
\end{aligned}$$

we obtain the expression of  $\Delta_{\mathbf{k}}$  in Eq.(4). Finally, the energy of the superconducting condensate,  $H_Q$ , is given by

$$H_Q = \frac{N}{U} |\Delta_S|^2 + \frac{4N}{V} |\Delta_{x^2-y^2}|^2 + \frac{4N}{Z} |\Delta_{xy}|^2 . \quad (\text{A6})$$

Minimizing the total energy with respect to  $\Delta_S$ ,  $\Delta_{x^2-y^2}$ , and  $\Delta_{xy}$ , we obtain the self-consistent equations for the gap order parameter, given by

$$\begin{aligned}
\Delta_S &= \frac{U}{2N} \sum_{\mathbf{k}} \frac{\Delta_S}{\epsilon_{\mathbf{k}}} \varphi(\epsilon_{\mathbf{k}}) \\
\Delta_{x^2-y^2} &= \frac{V}{2N} \sum_{\mathbf{k}} \frac{\Delta_{x^2-y^2} [\cos(k_x) - \cos(k_y)]^2}{\epsilon_{\mathbf{k}}} \varphi(\epsilon_{\mathbf{k}}) \\
\Delta_{xy} &= \frac{2Z}{N} \sum_{\mathbf{k}} \frac{\Delta_{xy} \sin^2(k_x) \sin^2(k_y)}{\epsilon_{\mathbf{k}}} \varphi(\epsilon_{\mathbf{k}}) , \quad (\text{A7})
\end{aligned}$$

with  $\epsilon_{\mathbf{k}} = \sqrt{\xi_{\mathbf{k}}^2 + |\Delta_{\mathbf{k}}|^2}$  and  $\varphi(\epsilon_{\mathbf{k}}) = f(-\epsilon_{\mathbf{k}}) - f(\epsilon_{\mathbf{k}})$ , with  $f(\epsilon_{\mathbf{k}})$  being Fermi distribution function.

From the self-consistent equations in Eqs.(A7) (taken in the zero-temperature limit) we have derived the phase diagram discussed in the main text.

## Appendix B: Relaxation dynamics following a sudden quench on $\Delta_{\mathbf{k}}(t)$

In this appendix we present a simplified version of the approach we used throughout our paper. Specifically, rather than quenching, at  $t = 0$ , the interaction strengths, we directly quench the superconducting order parameter, so that it takes the form

$$\hat{\Delta}_{\mathbf{k}}(t) = \Delta_{\mathbf{k}}^{(0)}\theta(-t) + \Delta_{\mathbf{k}}\theta(t) \quad . \quad (\text{B1})$$

As a result of giving up self consistency, for  $t > 0$  Eqs.(11) become purely linear and simplify to

$$\begin{aligned} \frac{d\nu_{\mathbf{k}}(t)}{dt} &= -2g\nu_{\mathbf{k}}(t) + \frac{g\xi_{\mathbf{k}}}{\epsilon_{\mathbf{k}}} + 2\Im m[\Delta_{\mathbf{k}}[f_{\mathbf{k}}(t)]^*] \\ \frac{df_{\mathbf{k}}(t)}{dt} &= -2(g + i\xi_{\mathbf{k}})f_{\mathbf{k}}(t) + 2i\Delta_{\mathbf{k}}\nu_{\mathbf{k}}(t) + \frac{g\Delta_{\mathbf{k}}}{\epsilon_{\mathbf{k}}} \end{aligned} \quad , (\text{B2})$$

with  $\epsilon_{\mathbf{k}} = \sqrt{\xi_{\mathbf{k}}^2 + |\Delta_{\mathbf{k}}|^2}$  and the initial conditions given by

$$\begin{aligned} \nu_{\mathbf{k}}(t=0) &= \frac{\xi_{\mathbf{k}}}{\epsilon_{\mathbf{k}}^{(0)}} \\ f_{\mathbf{k}}(t=0) &= \frac{\Delta_{\mathbf{k}}^{(0)}}{\epsilon_{\mathbf{k}}^{(0)}} \end{aligned} \quad , \quad (\text{B3})$$

with  $\epsilon_{\mathbf{k}}^{(0)} = \sqrt{\xi_{\mathbf{k}}^2 + |\Delta_{\mathbf{k}}^{(0)}|^2}$ . We may now readily solve Eqs.(B2) in terms of the Laplace transforms of  $\nu_{\mathbf{k}}(t)$  and  $f_{\mathbf{k}}(t)$ . As a result, we obtain

$$\begin{aligned} \nu_{\mathbf{k}}(z) &= \frac{g\xi_{\mathbf{k}}}{\epsilon_{\mathbf{k}}z(z+2g)} + \left[ \frac{(z+2g)\{2\Im m\{[f_{\mathbf{k}}(0)]^*\Delta_{\mathbf{k}}\} + (z+2g)\nu_{\mathbf{k}}(0)\} + 4\xi_{\mathbf{k}}\Re e\{[f_{\mathbf{k}}(0)]^*\Delta_{\mathbf{k}}\} + 4\nu_{\mathbf{k}}(0)\xi_{\mathbf{k}}^2}{(z+2g)[(z+2g)^2 + 4\epsilon_{\mathbf{k}}^2]} \right] \\ f_{\mathbf{k}}(z) &= \frac{g\Delta_{\mathbf{k}}}{\epsilon_{\mathbf{k}}z(z+2g)} + \left[ \frac{f_{\mathbf{k}}(0)(2|\Delta_{\mathbf{k}}|^2 + (z+2g)(z+2g-2i\xi_{\mathbf{k}})) + 2\Delta_{\mathbf{k}}(\Delta_{\mathbf{k}}[f_{\mathbf{k}}(0)]^* + i\nu_{\mathbf{k}}(0)(z+2g-2i\xi_{\mathbf{k}}))}{(z+2g)[(z+2g)^2 + 4\epsilon_{\mathbf{k}}^2]} \right] \end{aligned} \quad (\text{B4})$$

In the three cases we are investigating here, the Laplace transforms of the superconducting gap,  $\Delta_S(z)$ ,  $\Delta_{x^2-y^2}(z)$ , and  $\Delta_{xy}(z)$ , are given by

$$\begin{aligned} \Delta_S(z) &= \frac{U}{2N} \sum_{\mathbf{k}} f_{\mathbf{k}}(z) \\ \Delta_{x^2-y^2}(z) &= \frac{V}{2N} \sum_{\mathbf{k}} \{\cos(k_x) - \cos(k_y)\} f_{\mathbf{k}}(z) \\ \Delta_{xy}(z) &= \frac{2iZ}{2N} \sum_{\mathbf{k}} \sin(k_x) \sin(k_y) f_{\mathbf{k}}(z) \quad . \quad (\text{B5}) \end{aligned}$$

Using Eqs.(B4) and going through Eqs.(B5), we can readily compute the position of the poles of the Laplace transforms of the superconducting gaps, which provide us with the relevant informations concerning the gap dynamics. To do so, we first of all replace  $\nu_{\mathbf{k}}(0)$  and  $f_{\mathbf{k}}(0)$  with their expressions in Eqs.(B3), by setting

$$\begin{aligned} \Delta_{\mathbf{k}}^{(0)} &= \Delta_S^{(0)} + 2\Delta_{x^2-y^2}^{(0)}[\cos(k_x) - \cos(k_y)] \\ &\quad - 4i\Delta_{xy}^{(0)} \sin(k_x) \sin(k_y) \\ \epsilon_{\mathbf{k}}^{(0)} &= \sqrt{\xi_{\mathbf{k}}^2 + |\Delta_{\mathbf{k}}^{(0)}|^2} \quad . \quad (\text{B6}) \end{aligned}$$

Moreover, we also set

$$\begin{aligned} \Delta_{\mathbf{k}}(z) &= \Delta_S(z) + 2\Delta_{x^2-y^2}(z)[\cos(k_x) - \cos(k_y)] \\ &\quad - 4i\Delta_{xy}(z) \sin(k_x) \sin(k_y) \quad . \quad (\text{B7}) \end{aligned}$$

From the explicit expression of  $f_{\mathbf{k}}(z)$  in Eqs.(B4) we can infer the relaxation dynamics of the superconducting order parameter for  $t \geq 0$ . Indeed, we readily identify two

single poles at  $z = 0$  and at  $z = -2g$ . The former one determines the asymptotic value of the superconducting gap. Taking the corresponding residue and employing the time-dependent version of Eqs.(B5), we readily find that, from the pole at  $z = 0$ , the superconducting order parameter as  $t \rightarrow \infty$  takes a contribution equal to the after-the-quench value. An additional simple pole takes place at  $z = -2g$ , which corresponds to a damping of the corresponding contribution to  $\Delta_{\mathbf{k}}(t)$  as  $e^{-2gt}$ . Finally, an additional complex pole is expected to arise at  $z = -2g + i\omega_*$ , with  $\omega_*$  determined by the integration over  $d^2k$ : this determines again an exponential damping of the corresponding contribution to the superconducting gap over a time scale  $\sim (2g)^{-1}$  on top of an oscillating modulation with frequency  $\omega_*$ . Apparently, as long as  $g > 0$ , all the contributions are washed out by the exponential damping, except the ones entering the after-the-quench  $\Delta_{\mathbf{k}}$ , according to Eq. (B7). As  $g \rightarrow 0$  the asymptotic behavior becomes more involuted, also depending on the symmetry of the order parameter. From the above discussion, we expect that, when only a single interaction strength is different from zero, the relaxation time scale of the corresponding order parameter is independent of its symmetry as, in fact, witnessed by the results in Fig. 5.

- [2] C. L. Smallwood, W. Zhang, T. L. Miller, C. Jozwiak, H. Eisaki, D.-H. Lee, and A. Lanzara, *Phys. Rev. B* **89**, 115126 (2014).
- [3] F. Peronaci, M. Schiró, and M. Capone, *Phys. Rev. Lett.* **115**, 257001 (2015).
- [4] A. D. Caviglia, R. Scherwitzl, P. Popovich, W. Hu, H. Bromberger, R. Singla, M. Mitrano, M. C. Hoffmann, S. Kaiser, P. Zubko, S. Gariglio, J.-M. Triscone, M. Först, and A. Cavalleri, *Phys. Rev. Lett.* **108**, 136801 (2012).
- [5] A. Nava, C. Giannetti, A. Georges, E. Tosatti, and M. Fabrizio, *Nature Physics* **14**, 154 (2018).
- [6] P. A. Lee, N. Nagaosa, and X.-G. Wen, *Rev. Mod. Phys.* **78**, 17 (2006).
- [7] P. André, M. Schiró, and M. Fabrizio, *Phys. Rev. B* **85**, 205118 (2012).
- [8] M. Sandri and M. Fabrizio, *Phys. Rev. B* **91**, 115102 (2015).
- [9] W. Fu, L.-Y. Hung, and S. Sachdev, *Phys. Rev. B* **90**, 024506 (2014).
- [10] A. A. Zvyagin, *Low Temperature Physics* **42**, 971 (2016).
- [11] M. Heyl, *Reports on Progress in Physics* **81**, 054001 (2018).
- [12] M. Heyl, *Europhysics Letters* **125**, 26001 (2019).
- [13] G. Mazza, *Phys. Rev. B* **96**, 205110 (2017).
- [14] H.-P. Breuer and F. Petruccione, *The Theory of Open Quantum Systems* (Oxford University Press, 2002).
- [15] M. M. Wilde, *Quantum Information Theory* (Cambridge University Press, 2013).
- [16] A. Nava and M. Fabrizio, *Phys. Rev. B* **100**, 125102 (2019).
- [17] D. Manzano, *AIP Advances* **10** (2020), 025106.
- [18] A. Nava and M. Fabrizio, *SciPost Phys.* **12**, 014 (2022).
- [19] C. Artiago, A. Nava, and M. Fabrizio, *Phys. Rev. B* **107**, 104201 (2023).
- [20] G. Mazza and M. Schirò, *Phys. Rev. A* **107**, L051301 (2023).
- [21] T. Cui, X. Yang, C. Vaswani, J. Wang, R. M. Fernandes, and P. P. Orth, *Phys. Rev. B* **100**, 054504 (2019).
- [22] M. Heyl, A. Polkovnikov, and S. Kehrein, *Phys. Rev. Lett.* **110**, 135704 (2013).
- [23] P. Jurcevic, H. Shen, P. Hauke, C. Maier, T. Brydges, C. Hempel, B. P. Lanyon, M. Heyl, R. Blatt, and C. F. Roos, *Phys. Rev. Lett.* **119**, 080501 (2017).
- [24] C.-M. Schmied, A. N. Mikheev, and T. Gasenzer, *International Journal of Modern Physics A* **34**, 1941006 (2019).
- [25] E. A. Yuzbashyan and M. Dzero, *Phys. Rev. Lett.* **96**, 230404 (2006).
- [26] M. Prüfer, P. Kunkel, H. Stobel, S. Lannig, D. Linne-  
mann, C.-M. Schmied, J. Berges, T. Gasenzer, and M. K. Oberthaler, *Nature* **563**, 217 (2018).
- [27] K. Yamamoto, M. Nakagawa, N. Tsuji, M. Ueda, and N. Kawakami, *Phys. Rev. Lett.* **127**, 055301 (2021).
- [28] D. Mondal and T. Nag, *Phys. Rev. B* **106**, 054308 (2022).
- [29] D. Mondal and T. Nag, *Phys. Rev. B* **107**, 184311 (2023).
- [30] F. Pollmann, S. Mukerjee, A. G. Green, and J. E. Moore, *Phys. Rev. E* **81**, 020101 (2010).
- [31] N. O. Abeling and S. Kehrein, *Phys. Rev. B* **93**, 104302 (2016).
- [32] U. Bhattacharya, S. Bandyopadhyay, and A. Dutta, *Phys. Rev. B* **96**, 180303 (2017).
- [33] J. Lang, B. Frank, and J. C. Halimeh, *Phys. Rev. B* **97**, 174401 (2018).
- [34] L.-N. Wu, J. Nettersheim, J. Feß, A. Schnell, S. Burgardt, S. Hiebel, D. Adam, A. Eckardt, and A. Widera, “Dynamical phase transition in an open quantum system,” (2022), arXiv:2208.05164 [cond-mat.quant-gas].
- [35] J. Biscaras, N. Bergeal, S. Hurand, C. Grossetête, A. Rastogi, R. C. Budhani, D. LeBoeuf, C. Proust, and J. Lesueur, *Phys. Rev. Lett.* **108**, 247004 (2012).
- [36] M. S. Scheurer and J. Schmalian, *Nature Communications* **6**, 6005 (2015).
- [37] C. A. Perroni, V. Cataudella, M. Salluzzo, M. Cuoco, and R. Citro, *Phys. Rev. B* **100**, 094526 (2019).
- [38] L. Lepori, D. Giuliano, A. Nava, and C. A. Perroni, *Phys. Rev. B* **104**, 134509 (2021).
- [39] A. Nava, C. A. Perroni, R. Egger, L. Lepori, and D. Giuliano, “Dissipation driven dynamical topological phase transitions in two-dimensional superconductors,” (2023), arXiv:2308.08265 [cond-mat.str-el].
- [40] R. B. Laughlin, *Phys. Rev. Lett.* **80**, 5188 (1998).
- [41] A. Ghosh and S. K. Adhikari, *Phys. Rev. B* **60**, 10401 (1999).
- [42] M. I. Salkola and J. R. Schrieffer, *Phys. Rev. B* **58**, R5952 (1998).
- [43] A. Ghosh and S. K. Adhikari, *Physica C: Superconductivity* **370**, 146 (2002).
- [44] N. Goldman, J. C. Budich, and P. Zoller, *Nature Physics* **12**, 639 (2016).
- [45] R. Micnas, J. Ranninger, and S. Robaszkiewicz, *Rev. Mod. Phys.* **62**, 113 (1990).
- [46] C. C. Tsuei and J. R. Kirtley, *Rev. Mod. Phys.* **72**, 969 (2000).
- [47] A. V. Balatsky, *Phys. Rev. Lett.* **80**, 1972 (1998).
- [48] L. P. Gor'kov and E. I. Rashba, *Phys. Rev. Lett.* **87**, 037004 (2001).
- [49] T. Chern, *AIP Advances* **6**, 085211 (2016).
- [50] M. Mitrano, A. Cantaluppi, D. Nicoletti, S. Kaiser, A. Perucchi, S. Lupi, P. Di Pietro, D. Pontiroli, M. Riccò, S. R. Clark, D. Jaksch, and A. Cavalleri, *Nature* **530**, 461 (2016).
- [51] I. H. Choi, S. G. Jeong, T. Min, J. Lee, W. S. Choi, and J. S. Lee, *Advanced Science* **10**, 2300012 (2023), <https://onlinelibrary.wiley.com/doi/pdf/10.1002/advs.202300012>.
- [52] J. Huang, Z. Yue, A. Baydin, H. Zhu, H. Nojiri, J. Kono, Y. He, and M. Yi, *Review of Scientific Instruments* **94**, 093902 (2023).
- [53] E. A. Yuzbashyan, V. B. Kuznetsov, and B. L. Altshuler, *Phys. Rev. B* **72**, 144524 (2005).
- [54] E. A. Yuzbashyan, O. Tsypliyatyev, and B. L. Altshuler, *Phys. Rev. Lett.* **96**, 097005 (2006).
- [55] A. Nava, M. Rossi, and D. Giuliano, *Phys. Rev. B* **103**, 115139 (2021).
- [56] A. Nava, G. Campagnano, P. Sodano, and D. Giuliano, *Phys. Rev. B* **107**, 035113 (2023).
- [57] K. B. Efetov, I. A. Garifullin, A. F. Volkov, and K. Westerholt, “Proximity effects in ferromagnet/superconductor heterostructures,” in *Magnetic Heterostructures: Advances and Perspectives in Spinstruct* edited by H. Zabel and S. D. Bader (Springer Berlin Heidelberg, Berlin, Heidelberg, 2008) pp. 251–290.
- [58] B. Mera, C. Vlachou, N. Paunković, V. R. Vieira, and O. Viyuela, *Phys. Rev. B* **97**, 094110 (2018).
- [59] P. Zanardi and N. Paunković, *Phys. Rev. E* **74**, 031123 (2006).
- [60] H. T. Quan, Z. Song, X. F. Liu, P. Zanardi, and C. P. Sun, *Phys. Rev. Lett.* **96**, 140604 (2006).

- [61] Z. Lu and O. Raz, Proc. Nat. A. of Sciences **114**, 5083 (2017). Nuclear Physics B **960**, 115192 (2020).
- [62] A. Bácsi and B. Dóra, Phys. Rev. B **107**, 125149 (2023). [65] D. Giuliano, L. Lepori, and A. Nava, Phys. Rev. B **101**, 195140 (2020).
- [63] D. Guerci and A. Nava, Physica E **134**, 114895 (2021).
- [64] D. Giuliano, A. Nava, and P. Sodano,